Mullite Ceramic from Diphasic Precursor Powder

M. Tech (R) Thesis

Rupali Singh

DEPARTMENT OF CERAMIC ENGINEERING

2013-15

NIT ROURKELA

Mullite Ceramic from Diphasic Precursor Powder

A THESIS SUBMITTED IN PARTIAL FULFILLMENT OF THE REQUIREMENT FOR THE DEGREE OF

Master of Technology (Research)

Submitted by

Rupali Singh

Roll No. 612CR3009

Under the guidance of

Prof. Sunipa Bhattacharyya

Department Of Ceramic Engineering

National Institute of Technology

Rourkela, Orissa- 769008

(2013-2015)

CERTIFICATE

This is to certify that the thesis entitled, **"Mullite Ceramic from Diphasic Precursor Powder"**, submitted by **Ms. Rupali Singh** carried out in **National Institute of Technology, Rourkela**, in partial fulfilment of the requirements for the award of **Master of Technology by Research** Degree in **Ceramic Engineering,** is an authentic work carried out by her under my supervision and guidance.

To the best of my knowledge, the matter embodied in the thesis has not been submitted to any other University/ Institute for the award of any degree or diploma.

Prof. Sunipa Bhattacharyya

Department of Ceramic Engineering

National Institute of Technology

Rourkela-769008.

ACKNOWLEDGEMENT

It is a genuine pleasure to express my deep sense of thanks and gratitude to my mentor and guide **Prof. (Mrs.) Sunipa Bhattacharyya,** Department of Ceramic Engineering, NIT Rourkela. Her dedication and keen interest above all her overwhelming attitude to help her students had been solely and mainly responsible for completing my work. Her timely and scholarly advice, her inspiring guidance, constructive criticism, valuable suggestion throughout and scientific approach have helped me to a very great extent to accomplish this task. It has been a greatly enriching experience to me to work under her authoritative guidance.

I owe a deep sense of gratitude Prof. B. B. Nayak Current Head, Department of Ceramic Engineering, and S. K. Pratihar Previous Head, Department of Ceramic Engineering, NIT Rourkela for providing me all the departmental facilities and other technical suggestions required for the completion of the thesis.

My sincere thanks are extended to P. K Mohanthy, Subhabrata Chakraborty, Arvind Kumar for helping and encouragements have been especially valuable in greater part of this dissertation.

I also take this opportunity to thanks all other teachers, staff and colleagues who have constantly helped me grow, learn and mature both personally and professionally throughout the process. I thank profusely all the MSC Members for their kind help and co-operation and timely advice throughout my study period.

A big thanks goes to my dearest friends who have always supported, guided and even criticized me, always for the right reasons and have helped me stay sane throughout this and every other chapter of my life. I greatly value their friendship and deeply appreciate their belief in me. Special thanks to all the new friends from M.Tech (R). I have made without whom the journey wouldn't have been so interesting and memorable!

Most importantly, none of this would have happened without the love and patience of my family-my mother to whom this dissertation is dedicated. I would like to express my heart-felt gratitude to my family.

Rupali Singh

Content

LIST OF FIGURES

LIST OF TABLES

LIST OF ABBREVIATIONS

D Average particle diameter

ρ True density of material

s Specific surface area

σ The maximum stress

P The fracture load

L Span length

W Width

d Breadth of the specimen

G Gibbsite

B Bayerite

γ Gamma Alumina

δ Delta Alumina

θ Theta Alumina

κ’ Kappa Alumina

m Mullite (73-1253)

M Mullite (15-0776)

R Rutile

ABSTRACT

The use of mullite as a ceramic material proliferate from the field of conventional ceramic to the most advanced structural and functional area of ceramic due to its many advantageous properties. The properties of a sintered mullite ceramic are very much dependent on the type of processing route by which powder precursor was prepared.

In the present work, the stoichiometric diphasic mullite precursor powder was prepared by reverse addition technique using fume silica and aluminium nitrate nonahydrate as raw material. The effects of solution pH on the properties of the prepared powder have been investigated. The precursor powder made at ph-6, pH-8 and pH-10 were studied by TG-DSC analysis to know about the thermal decomposition behavior. Phase analysis of the precursor powder and calcined powder at different temperatures was done by XRD study. The presence of the different functional group in the precursor powder and calcined powder is confirmed by the FTIR study. The particle morphology, tendency of agglomeration and surface area, was investigated by microstructure analysis, particle size distribution and surface area analysis respectively. It was found that though the desired mullite phase formation is not very much affected by the variation of solution pH but the other properties are pH dependent.

The precursor powder formed at pH-8 exhibited better properties compared to the other batches. Therefore, the sintering study of the precursor powder in the presence of the different quantity of TiO_2 additive is continued with that powder only. Samples made from different batches were sintered at three different temperatures i.e. 1450 $^{\circ}$C, 1550 $^{\circ}$C and 1650 $^{\circ}$C under ambient atmosphere. The sintered pellets were characterized with respect to shrinkage, percent apparent porosity and bulk density. The phases formed in the sintered pellets were analyzed by X-Ray diffraction study. Morphology and microstructure were evaluated by FESEM.

Key words: Mullite, Diphasic powder, Solution pH, Thermal study, Phase analysis, Morphology, Sintering additive, Densification, Strength, Microstructure.

CHAPTER 1

INTRODUCTION

1.1 Introduction

Mullite, having composition $3Al_2O_3.2SiO_2$, is a widely studied stable crystalline phase in the binary alumina-silica phase diagram. Its excellent properties like its low coefficient of thermal expansion, good thermal shock resistance, creep resistance, high chemical, and thermal stability make it an excellent ceramic material for the high-temperature structural application [1.1, 1.2]. Phase pure polycrystalline mullite can retain a significant portion of its room temperature strength up to 1500 ˚C.

Mullite can be synthesized broadly by two methods one is traditional or conventional processing method and other is the chemical processing method. In the traditional method, mullite is produced from some naturally occurring alumina-silicate minerals like sillimanite, kaolinite, etc. [1.1, 1.2]. The problem related to this route is the high-temperature requirement for completing the solid state reaction. Here mineral sources are used as starting material, so the possibility of the presence of an impurity in the desired product is high. When the impurity level is more, then there is a possibility of the glassy phase formation at a higher temperature that reduces the strength of the desired product. The probability of contamination can be avoided if very high purity oxide of Si and Al are used as starting material. But, here also required sintering temperature is high greater than 1650 ˚C and mixing occurs in micrometre level only [1.3, 1.4]. In conventional or traditional ceramic industries, the motive of cost-effective production cannot be fulfilled by using these high purity oxides due to their very high cost. However, in case of chemical processing intimate mixing of starting material is possible which ultimately decrease the mullite phase formation temperature. Different chemical routes are used to prepare mullite precursor powders like sol-gel, co-precipitation, hydrolysis, spray pyrolysis, chemical vapour deposition (CVD) techniques, etc.

On the basis of homogeneities mullite, precursor powder can be divided into two types, monophasic precursor powder and diphasic precursor powder. In case of monophasic precursor powder, where homogeneity is very high at the atomic level the direct mullitization is possible at a temperature as lower as 980 °C. In case of diphasic precursor powder, the homogeneity is in the nanometer or micrometer level, so the mullite formation temperature increases to more than 1200 ˚C and it forms by means of a transient Al_2O_3 phase [1.5, 1.6]. It is known that an earlier mullite formation hampers the densification process. This behaviour suggests that densification before starting of mullitization is the best method to achieving better densities [1.7]. Though the diphasic precursor delayed the mullite formation, but here the heat of reaction of different phases or probably the heat of mixing in an amorphous system provides extra energy for densification process [1.8]. Thus, the diphasic gel is a better option for producing sintered mullite ceramic. The pH of the diphasic gel influences very much the phase formation temperature and the morphology of the mullite formed. In the acidic pH mullite formation occurs around 1200 ˚C and needle-shaped mullite formed whereas in alkaline pH mullite formation occurs above 1200 ˚C and rod-like or granular shaped mullite formed [1.9, 1.10]. The acicular mullite retarded the densification process. The acicular nature of the mullite generates large pores within the structure and with that stiff mullite structure densification is difficult.

In case of diphasic aluminosilicate gel mullite formation is controlled by dissolution-precipitation reactions. In this reaction, alumina dissolves first in the co-existing silica-rich liquid phase, so the ease of glass formation and alumina dissolution are the two important factors that control mullite formation. When additives are added then, those additives are helped in the liquid phase formation and this less viscous liquid phase helps in both phase formation and densification. Many researchers tried different additive like MgO, La_2O_3, Y_2O_3, B_2O_3, CeO_2, etc., most of which form a low-temperature eutectic with the Al_2O_3-SiO_2

system and help sintering by removal of pores. Though this liquid phase formation is beneficial for sintering but the presence of those glassy zones at higher temperature is harmful to maintain high-temperature strength. Titania doped mullite had been prepared and characterized by several authors [1.11, 1.12]. For single phase mullite gel, they showed that as the titania content increases the crystallization temperature reduces [1.12]. For sol-gel processed mullite bending strength increases with increasing titania content [1.13]. The presence of titania improves the fracture strength and develop microstructure in which mullite grains are properly interlocked [1.12]. Thus, it can be said TiO_2 is a potential additive for mullite that helps in phase formation sintering and mechanical property improvement.

The importance of preparation methods for both pure and doped mullite has increased significantly in recent times. Coprecipitation is a method in which joint precipitation was done from the solution of difficultly soluble salt and their washing, drying, and calcination are followed. It is two type direct precipitation in which precipitator is added to the salt solution and inverse precipitation in which salt solution was poured into the precipitator. In the reverse method, the precipitate formed is more finely dispersed than the precipitate formed by the forward method which increases the solid state interaction and correspondingly decreases the sintering temperature [1.14]. In this work, we have tried to prepare the mullite precursor powder using aluminium nitrate nonahydrate and fumed silica as a starting material by reverse addition method at three different pH. The precursor powders formed were characterized by various techniques. The sintering study in the presence of the different amount of titania additive is also carried out.

References

[1.1] V. Viswabaskaran, F. D. Gnanam, M. Balasubramanian, Mullitisation behaviour of calcined clay- alumina mixture, Ceramics International, 29 (2003) 561-571.

[1.2] C.Y. Chen, G.S. Lan, and W.H. Tuan, Preparation of mullite by the reaction sintering of kaolinite and alumina, Journal of the European Ceramic Society, 20 (2000) 2519-2525.

[1.3] I.A. Aksay, D.M. Dobbs and M. Sarikaya, Mullite for Structural, Electronic and Optical applications, Journal of Am. Ceram. Soc., 74 (1991) 2343-2358.

[1.4] P.Kansal, R. M. Laine and Florence Babonneau, A processable mullite precursor prepared by reacting silica and aluminum hydroxide with triethanolamine in ethylene glycol: structural evolution on pyrolysis, Journal of Am. Ceram. Soc., 80 [10] (1997) 2597-2606.

[1.5] C. Gerardin, S. Sundaresan, J. Beziger and A. Navrotsky, Structural investigation and energetics of mullite formation from sol-gel precursors, Chem. Mater., 6 (1994) 160-170.

[1.6] Dong X. Li and W. J. Thomson, Effects of hydrolysis on the kinetics of high-temperature transformations in aluminosilicate gels, J. Am. Ceram Soc., 74 (1991) 574-578.

[1.7] Jihong She, Peter Mechnich, Martin Schmucker, Hartmut Schneider, Low-temperature reaction-sintering of mullite ceramics with an Y_2O_3 addition, Ceramics International, 27 (2001) 847-852.

[1.8] Saikat Maitra, Jagannath Roy, Effect of TiO_2 and V_2O_5 additives on chemical mullite, Advances in ceramic science and engineering, 2 [3] (2013) 130-133.

[1.9] Jae-Ean Lee, Jae-Won Kim, Yeon-Gil Jung, Chang-Yong Jo, Ungyu Paik, Effect of precursor pH and sintering temperature on synthesizing and morphology of sol-gel processed mullite, Ceramics International, 28 (2002) 935-940.

[1.10] Carla C. Osawa and Celso A. Bertran, Mullite formation from mixtures of alusmina and silica sols: Mechanism and pH effect, J. Braz. Chem. Soc., 16 (2005) 251-258.

[1.11] C. R. Green and J. White, Solid solubility of TiO_2 in mullite in system Al_2O_3-TiO_2-SiO_2, Trans. Br. Ceram. Soc., 73 [3] (1974) 73-75.

[1.12] Seong-Hyeon Hong and Gary L. Messing, Anisotropic Grain Growth in Diphasic-Gel-Derived Titania-Doped Mullite, J. Am. Ceram. Soc., 81 [5] (1998) 1269-1277.

[1.13] E. R. De Sola, Francisco Estevan, Javier Alarcon, Low-temperature Ti-containing 3:2 and 2:1 mullite nanocrystals from single-phase gels, Journal of the European ceramic society, 27 (2007) 2655-2663.

[1.14] N.M. Bobkova, I. V. Kavrus, E. V. Radion and F. Popovskaya, Formation of mullite obtained by coprecipitation, Glass and Ceramics, 55 (1998) 5-6.

CHAPTER 2
LITERATURE REVIEW

2. Literature review:-

2.1 Properties and Applications of Mullite:-

Mullite ceramic is enormously used in the field of electronic, optical and structural application [2.1, 2.2]. Aksay et. al. [2.1] has been investigated the structure, properties and application areas of mullite ceramic. Mullite is used for electronic applications due to its low dielectric constant (ε=6.5 at 1 MHz), high wiring density and low thermal expansion co-efficient (20/200 $^{\circ}$C=4×10^{-6} K^{-1}) [2.3, 2.4]. In the optical field, it is used due to its good transparency for mid-infrared light. It also has numerous physical and chemical properties like high temperature strength, high creep resistance, excellent thermal shock resistance, low thermal conductivity (k=2.0 $Wm^{-1}K^{-1}$), high thermal stability, good mechanical strength, good chemical stability etc which make it an excellent material for structural applications [2.1-2.4]. Some of the classical uses of mullite are in electrical furnace roof, hot metal mixers, low-frequency induction furnace, kiln setting slabs and linings of high-temperature reactors [2.2].

In 2008 Schneider et. al. [2.3] has described three types of polycrystalline mullite ceramics namely monolithic mullite ceramics, mullite coatings, mullite composites. Monolithic mullite ceramic is used for making tableware, porcelain, refractories, kiln furniture, catalytic converters etc. Mullite coatings are used to protect metals and ceramics from chemical degradation at high temperature. This type of surface coating known as environmental barrier coatings (EBC) which makes the material stable under certain conditions.

Mullite composites include mullite matrices and mullite fibres which increase the toughness of the system and reduce the brittleness property. These are used in the components and structures for gas turbine engines, high duty kiln furniture, burner tubes, and re-entry space vehicles. At present, it is highly used as a matrix material for high-temperature composite

developments, a substrate in multilayer packaging, protective coatings and infrared transparent windows.

2.2 Phase Diagram And Crystal Structure:-

Mullite is a stable crystalline phase in the binary alumina-silica phase diagram. Bowen and Grieg [2.5] in 1924 proposed the first alumina–silica phase diagram and showed that mullite $3Al_2O_3$-$2SiO_2$ (71.8 wt. % Al_2O_3) is the only compound that melts incongruently at 1810˚C. Shears and Archibald [2.6] in 1954, described that mullite having a solid solution range from $3Al_2O_3$-$2SiO_2$ (3:2 mullite) to $2Al_2O_3$-SiO_2 (2:1 mullite) melted congruently at approximately 1810 ˚C. Aramaki and Roy [2.7] in 1962, reported a solid solution range of mullite 71.8-74.3 wt% Al_2O_3 and congruent melting point that was supported by the position of the α-Al_2O_3, liquidus. They also identified that under metastable conditions the solid solution range was extended to 77.3 wt% of $A1_2O_3$. In the alumina-silica phase diagram, there are two key problems having controversy; Melting of mullite and Solid-solution range of mullite phase. The melting problem of mullite is related with the nucleation kinetics of mullite or alumina in alumina-silica melts. In 1975, Aksay and Pask [2.8] determined two different behaviours i.e. stable melting behaviour of mullite above 1800 ˚C and solid-solution range of mullite. According to them, under stable equilibrium condition mullite melts incongruently at 1828+/-10˚C and solid solution range 70.5 to 74.0 wt% Al_2O_3 below 1753˚C. After many of conflicting views on the Al_2O_3-SiO_2 diagram, Klug et. al. [2.9] published their SiO_2-Al_2O_3 phase diagram in 1987 as shown in figure 2.1 . They reported that mullite melted incongruently at 1890˚C and showed that above the eutectic point of 1587^{o}C, both the boundaries of mullite solid solution region shifted towards higher alumina content. Mullite formation starts from 58% Al_2O_3 (silica-rich region) to 75% Al_2O_3 (alumina-rich region) in alumina-silica system. The solid solution range varies from $3Al_2O_3.2SiO_2$ (3:2 mullite) to $2Al_2O_3.3SiO_2$ (2:1 mullite). The melting point of silica and alumina is around 1700˚C and

2000˚C respectively, so when the mullite is in the silica-rich region; its melting point is lower than the mullite in alumina rich region. The melting of mullite is incongruent at 1890˚C, but this temperature may change with the change in a composition of the $3Al_2O_3.2SiO_2$ system [2.10].

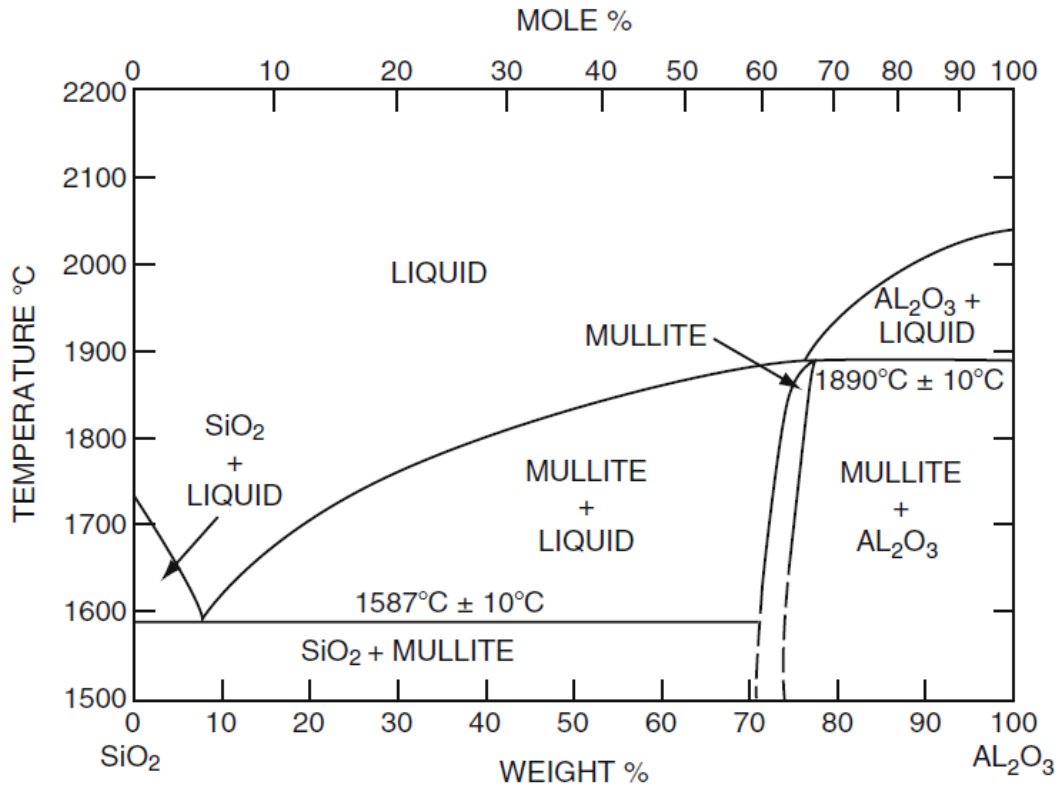

Figure 2.1 Phase Diagram of SiO_2-Al_2O_3 [2.9].

Mullite is intermediate in composition between Al_2O_3 and sillimanite [2.1]. The crystal structure of mullite is orthorhombic with space group Pbam and unit cell dimensions a=0.7540 nm, b= 0.7680 nm, c= 0.2885 nm (figure 2.2) [2.1, 2.2]. It is modified defect structure of sillimanite $Al_2O_3.SiO_2$ in which Si^{+4} ion are substituted by Al^{+3} ions in the tetrahedral site to get mullite stoichiometry [2.1].

$2Si^{+4} + O^{-2} = 2Al^{+3} + \Delta$ (Δ = oxygen vacancy)

It is usually represented by the formula $Al_2Al_{2+2x}Si_{2-2x}O_{10-x}$ where x denotes the fraction of vacancies per unit cell. Where, x=0 for sillimanite, x=0.25 for 3:2 mullite ($3Al_2O_3.2SiO_2$), x= 0.4 for 2:1 mullite ($2Al_2O_3.SiO_2$), x=0.57 for 3:1 mullite ($3Al_2O_3.SiO_2$). With increasing alumina content Si^{+4} is replaced by Al^{+3} and O^{-2} vacancies are created for charge neutrality.

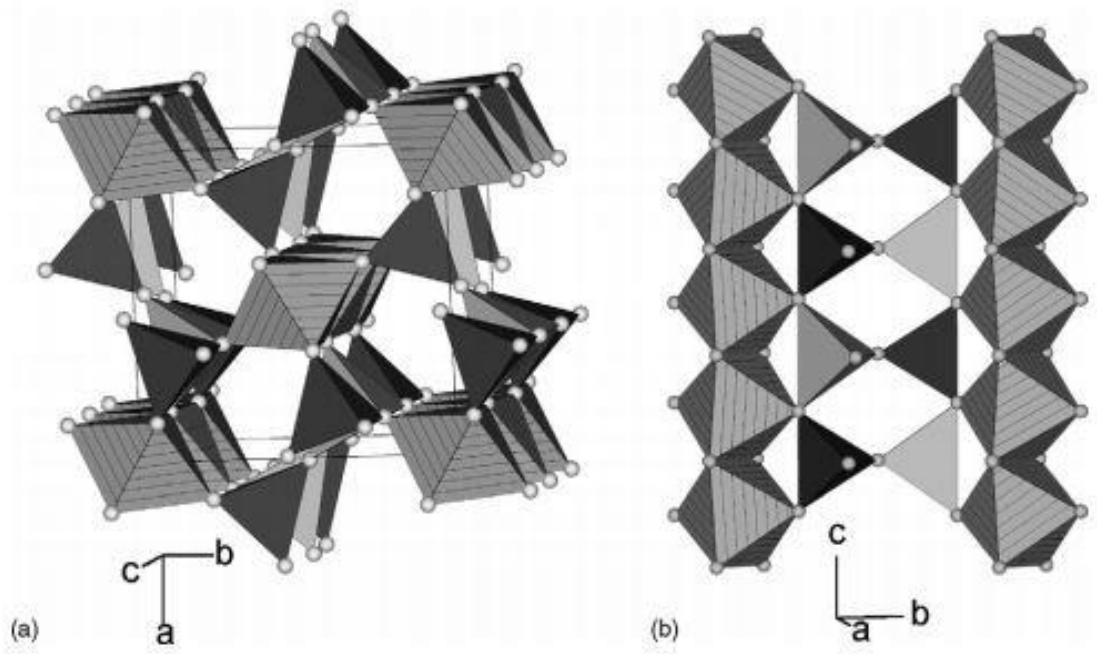

Figure 2.2 Structure of mullite [2.3].

2.3 Synthesis Processes:-

The synthesis of mullite precursor powder can be done either by conventional processing methods or chemical processing methods. In conventional or traditional processing, mullite precursor powder was formed from naturally occurring aluminosilicate minerals like sillimanite, kaolinite, clay, etc. Chen et. al. [2.11] in 2000, prepared mullite by reaction sintering method using kaolinite and alumina as raw material. This process required relatively high sintering temperature while the achieved density and strength were very low.

Viswabaskaran et. al. [2.4] in 2003, study the mullitization behaviour of three South Indian (Neyveli, Panruti and Udayarpalayam) calcined clays with three different alumina sources (reactive alumina, gibbsite and boehmite). They found that the calcined clay (metakaolin) samples showed higher strength and density in comparison to their uncalcined counter part. The microstructure also exhibited higher aspect ratio of mullite crystals. Among these three clay combinations, the calcined Neyveli clay and fine reactive alumina mixture was found to exhibit a better mullitisation behaviour compared to other combinations. The mullite synthesised using boehmite shows better microstructure due to purity, smaller particle size and homogeneous mixing with clays. However, the water loss in boehmite samples is high, that creates surface cracks resulting in poor strength.

Aksay et. al. [2.1] in 1991, disclosed that the main drawbacks of the traditional route was the presence of impurities in the desired product. The impurities can be prevented by the use of a very high purity oxide of Si and Al as a raw material.

Kansal et. al. [2.12] in 1997, synthesised mullite by using aluminum hydroxide hydrate and silicon dioxide and found that orthorhombic mullite formed at 1300 °C. Juliana Anggono [2.2] in 2005 classified mullite according to their preparation routes as (1) sinter-mullite, (2) fused-mullite (3) chemical-mullite (high-purity mullite). In conventional processing methods, mullite powders are shaped and sintered which is called 'sinter-mullite'. Fused-mullite is produced either by melting the raw materials in an electric furnace above 2000 °C with subsequent crystallisation of mullite during cooling of the bath or by Czochralski crystal growth techniques. Chemical-Mullite powders are prepared by different advanced processing methods, e.g. sol-gel, co-precipitation, hydrolysis, spray pyrolysis, chemical vapour deposition (CVD) techniques [2.2].

2.3.1 Combustion process:-

Chandran et. al. [2.13] in 1990, reported a low-temperature combustion process that yields mullite very rapidly compared to other processes. In this process, a mixture was prepared by using aluminium nitrate, fume silica and urea as raw material. The mixture was rapidly heated in a muffle furnace at a temperature of 500 °C, and it ignites to burn with a flame. The entire combustion process is over in less than 5 min. They claimed that this process was simple, safe, rapid, energetically favourable, technologically attractive and affordable.

2.3.2 Mechanochemical route:-

Temuujin et. al. [2.14] in 1998, discussed the mechanochemical route, in which the powders were ground in a pot mill at room temperature using a rotation speed of 400 rpm. In this process, gibbsite and amorphous silica were used as raw materials. This process promotes the formation of Al-O-Si bonds. This bond formation upgraded the homogeneity of the system and caused crystallization of spinel phase at about 980 °C. A further consequence of mechanochemical processing is low mullitization temperature. After mechanochemical processing, the surface excess hydroxyl groups formed in the starting material leads to a decrease in the mullitization temperature at about 150-200 °C. In 1998 [2.15], they repeat their previous work but using different raw materials i.e. gibbsite with silica gel, α-Al_2O_3 with silica gel and gibbsite with fused silica. They found that precursor prepared from gibbsite and silica gel transform into mullite at 1200 °C whereas other combinations transformed around 1400 °C. Incomplete mullitization found in precursors formed from gibbsite and fused silica. The substitution of α-alumina for gibbsite leads to the least reactive precursor.

2.3.3 Sol-Gel route:-

Sol-Gel is very important and widely used synthetic route of chemical processing to achieve good mixing and uniformity of starting materials. This uniform mixing results at the highly homogeneous distribution of components [2.16]. The essential features in comparison with solid state ceramic methods are high chemical homogeneity, lower processing temperatures, control of particles size and morphology, and the possibility of preparing new crystalline or non-crystalline materials [2.17]. Roy et. al. [2.18] in 2011, made diphasic mullite precursor powder by a sol-gel route using aluminium nitrate and silicic acid as raw materials. The precursor powder synthesized by this route produced highly pure and homogeneous material at a lower temperature. They found that the crystallization of mullite phase started after heating at 1200 °C and completed after heating at 1600 °C.

2.3.4 Precipitation route:-

Sugita et. al. [2.19] in 1998, prepared fine pure mullite powder by homogeneous precipitation route. Fumed silica, aluminium sulphate and ammonium bisulphate were used as a raw materials. This mullite precursor powder will transform quickly into crystalline mullite by heat treatment. Amorphous basic aluminium sulphate salt coated fumed silica can be produced by this method. According to them, this route is an inexpensive and efficient way to prepare the fine mullite powder. Okada et. al. [2.20] in 1986, made two kinds of xerogels by the slow and rapid hydrolysis process using TEOS and aluminium nitrate as raw material. Xerogel prepared by slow hydrolysis crystallised mullite directly from the amorphous state on firing whereas those formed by rapid hydrolysis crystallised to a spinel phase before mullite formation. The authors found that spinel phase formation was started after 980 °C and formation of mullite occurred at 1150 °C.

Lee et. al. [2.21] in 1992, prepared diphasic mullite powder by direct co-precipitation process using the mixed oxide solution of colloidal silica and aluminium nitrate as raw material. The

ammonia solution was used as a precipitant in this process. With the increase in temperature, the pseudo boehmite and amorphous silica reacted independently, up to the mullite formation. The composition also varied from alumina-rich to the stoichiometric composition of mullite (3:2) as the temperature rises. Bobkova et. al. [2.22] in 1998, investigated the direct and indirect co-precipitation route and studied the effect of precipitation pH, the order of precipitation and synthesis route. They established that at pH 6, the formation of mullite start at the temperature of 900 °C for the inverse precipitated mullite whereas for direct precipitation mullite formation were started at 1100 °C. Thus, the inverse order precipitation process proceeds more intensely. However, with pH 7-8 synthesis of mullite proceeds via a transitional phase or intermediate crystalline phase and mullitization occurred in the range of 1300-1400 °C.

2.3.5 Effect of pH:-

Solution pH has an important effect on mullitization. Chakravorty [2.23] in 1994, investigated, the behaviour of mullite formation at different pH condition. They found that when the pH was in the range of 3-4.5 direct mullite crystallization occurs at 980 °C. Whereas, if pH was lower than 1 or around 14 then the precursor powder does not show a 980 °C exotherm but forms γ-Al_2O_3 or the intermediate Si-Al spinel phase and the mullite formation was occurred at 1330 °C.

AnilKumar et. al. [2.24] in 1997, prepared gels with the pH value 3.5, 5.5 and 8, the total weight loss in all the gels were nearly same (72%) and with increasing pH decrease was of 2%. The precursor gel prepared at low pH conditions formed crystalline mullite at 1250 °C and at higher pH α-Al_2O_3 was a major phase, this α-Al_2O_3 phase was retained even at high-temperature 1500 °C.

Lee et. al. [2.25] in 2002, described that the gel in acid sample was transparent whereas gel in basic sample was opaque that indicates the rate of gelation and physicochemical nature of the gels were dependent upon the precursor pH. When the precursor has pH≤ 2 (acidic sample), it shows high aspect ratio at high sintering temperature with total wt. loss around 28%. Whereas, when the precursor pH≥8 (basic sample), it transforms into rod-like or granular shape with increasing sintering temperature. But wt. loss in the basic sample is higher ~ 51% than the acidic sample, and the alumina silica sol can form relatively less network and larger primary particles in higher pH. Osawa et. al. [2.26] in 2005, reported that the pH of mullite sample determines the surfaces charges of particle and affects their interactions and distributions. They found that when mullite precursor formed by 3:1 molar ratio, the pH played an important role in interaction between alumina and silica particles whereas sols prepared by 1:3 molar ratio is not affected by pH. At pH 1 octahedral Al^{+3} ions predominated in the alumina sol while at pH~6 tetrahedral coordinated Al^{+3} ions predominated in the sol.

2.3.6 Monophasic and Diphasic powder:-

According to the chemical homogeneities or short-range atomic arrangement mullite precursor powder can be divided into two categories, monophasic precursor powder and diphasic precursor powder [2.27, 2.28].

In monophasic [2.29] precursor powder the mixing of alumina and silica was achieved at the molecular level, and entirely amorphous phase is converted into crystalline mullite at 980 °C by a nucleation controlled process. These precursor powder are formed by the replacement of silicon in the silica three-dimensional network, by atoms and hydrolyzed aluminum molecules, leading to bonds Al–O–Si. This bond formation is similar to those bond formed during the mullite crystallization stage [2.30 - 2.32].

In diphasic [2.29] precursor powder the mixing of alumina-silica was occurred at nano-scaled level. The mullite forms through a diffusion-controlled reaction between either transition aluminas (δ, γ, θ) and amorphous silica or Al-Si spinel and amorphous silica at 1150-1350 °C.

2.4 Densification of mullite precursor powder:-

Sundaresan et. al. [2.33] in 1991, described that in the mullite precursors among the two pure phases one is transition alumina while the other is amorphous silica. Alumina particles dissolve in the amorphous silica phase, under thermal treatment, leading to the formation of an aluminosilicate matrix. Mullite nuclei are formed only when the alumina concentration in the matrix exceeds a critical nucleation concentration. These nuclei grow is controlled by the alumina particle incorporation or by the alumina dissolution in the amorphous phase.

Highly pure, dense mullite ceramics can be achieved by various routes like solid state sintering of mullite precursor powder and the reaction sintering of silica, alumina. Solid state sintering requires higher temperature due to the lower rate of silicon and aluminium ion interdiffusion [2.34]. Here agglomerate formation during drying and calcination is another factor that affect densification. In reaction sintering two processes, reaction and densification occur simultaneously and in most cases they are mutually favourable. But in case of mullite formation high activation enthalpy requirement makes the densification process difficult [2.35]. Sintering of mullite can be done by different methods according to the raw material used and the method of synthesis.

Rodrigo et. al. [2.35] in 1985 suggested that the best way to achieve high-density mullite ceramic is reaction sintering. They obtained the high purity dense mullite by using amorphous silicon dioxide and α-aluminium oxide. They found that for the stoichiometric $3A1_2O_3.2SiO_2$ (mullite), 97% densification can be achieved and for compositions close to

75.0 wt % Al_2O_3, it was minimum, in which excessive grain growth occurs. Kara et. al. [2.34] in 1996 investigated two structurally different diphasic mullite precursor powders. The first one derived from boehmite and colloidal silica at around 1250 °C. The second one, derived from aluminium sulfate and colloidal silica at around 1200 °C. They claimed that sinterability was dependent on the calcination temperature of the powder. They reported that if calcination of the powders was below to the mullite formation temperature~1000 °C then it reduces the weight loss and avoid excessive shrinkage during sintering which gives a positive effect on the sample. But when it was calcined above mullite formation temperature~1200 °C, it reduced the sinterability of the sample. Ebadzadeh [2.36] in 2003, prepared mullite by using aluminium sulphate/boehmite and colloidal silica as the starting material. They studied the effect of those raw materials on mullitization, densification, microstructure and mechanical properties of the prepared product. Their observations were that mullitization temperature decreased by using aluminium sulphate and colloidal silica as raw materials and achieved mechanical properties were very low. Whereas mullite derived from boehmite and colloidal silica showed improvement in densification and mechanical properties due to the higher particle packing density, retarded crystallization and lower calcination temperature.

Amutharani et. al. [2.37] in 1999, used aluminium nitrate nanohydrate and ethyl silicate for mullite synthesis. They achieved only 88.5% of the theoretical density after sintering at 1600 °C for 3 hrs. They studied the effect of different additives like SrO and Clay and found that additive modifies the density and other properties of the sintered sample. They reported that clay is a suitable sintering aid for mullite, and it helped to increase density up to 95% of T.D at 1450 °C. Again in 2001, they studied the microstructure of SrO doped mullite and clay doped mullite. The SrO doped samples showed a duplex microstructure of fine equiaxed and anisotropic grain morphology while the sintered clay doped samples show equiaxed and acicular morphology [2.38].

She et. al. [2.39] in 2001, reported the fabrication of low-temperature mullite ceramics from α-Al_2O_3 and quartz, using Y_2O_3 as sintering aids. The densification behaviour was investigated as a function of the Y_2O_3 content, sintering temperature and holding time. They observed that mullitization occurs via a nucleation and growth mechanism within a yttrious aluminosilicate glass, and during this densification process, lattice and grain-boundary diffusion becomes important. Moreover, they reported that the incorporation of mullite seeds enhanced both mullitization and densification process. Finally, they showed, 15 mol% Y_2O_3-doped and 5 mol% mullite-seeded specimens can be sintered for 5 hours to almost full density. Roy et. al. [2.40] in 2010 prepared mullite by using aluminium nitrate and silicic acid as raw materials and studied the effect of copper oxide dopant. They reported that the presence of copper oxide increased the densification as well as improved the mechanical properties. This improvement is due to the liquid phase formation that reduces the stress and help to form more interlocked crystalline phases.

2.5 Effect of sintering additive

Hong et. al. [2.41] in 1997 prepared mullite poeder precursor by a sol-gel route using boehmite and silica sol. They studied the effect of different dopants like P_2O_5, TiO_2, and B_2O_3 and found that the mullite formation temperature decreased with TiO_2 doping and the rate of transformation increased with decreasing particle size of TiO_2. They investigated that the mullite formation temperature depends on the initial particle size of titania due to the enhanced dissolution rate of titania into amorphous silica phase before mullite transformation, as well as a decrease in glass viscosity. Sola et. al. [2.42] in 2007, synthesized mullite from aluminium nitrate and tetraethylorthosilicate. They studied the effect of TiO_2 additive on the densification and other properties of mullite. They observed that the increment in titania concentration reduced the crystallization temperature of single phase mullite gel. They examined the microstructure and found that in the presence of nominal

amount of titanium oxide the anisotropic growth of mullite crystals occurred. They also claimed that the anisotropic growth is temperature dependent and occurred above 1400 °C. Naga et. al. [2.43] in 2011, prepared mullite through the sol-gel process using aluminium nitrate nonahydrate and tetraethyl orthosilicate as raw materials. They studied the effect of TiO_2 doping and reported the enhanced bulk density and bending strength with reduced porosity in TiO_2 doped mullite. The rod-like anisotropic mullite grains were developed in titania-doped mullite bodies sintered at 1650 °C. Maitra et. al. [2.44] in 2013, prepared mullite gel by using aluminium nitrate nonahydrate and liquid sodium silicate as a raw materials. They used titanium dioxide as a sintering additive. They reported that due to the addition of TiO_2 additive densification and other properties were enhanced. TiO_2 decompose into Al_2TiO_5 phase at a higher temperature which helps in the densification of mullite. The mechanical properties were also improved significantly due to improved microstructure and favourable phase compositions.

2.6 Summary of contributions

The extensive literature review shows that no attempt has been made for the preparation of diphasic mullite precursor powder by reverse addition technique using aluminium nitrate salt and fumed silica. The studies related to the effect of solution pH on the mullite phase formation are also limited to the lower pH range. The investigations to find out the effect of TiO_2 on densification of monophasic mullite gel have already covered, but the impact of that additive on diphasic powder has not much explored. Based on the findings mentioned above the work plan of this thesis is outlined.

2.7 Thesis Objective

- To synthesise diphasic mullite precursor powder using reverse addition method.
- To study the effect of the pH change on the phase formation of mullite precursor powder.

- To study the effect of titania additive on phase formation and densification of mullite ceramic derived from this diphasic precursor powder.

References

[2.1] I. A. Aksay, D. M. Dobbs and M. Sarikaya, Mullite for Structural, Electronic and Optical applications, Journal of Am. Ceram. Soc., 74 (1991) 2343-2358.

[2.2] J. Anggono, Mullite Ceramics: Its Properties, Structure and Synthesis, Journal Teknik Mesin, 7 [2] (2005) 1-10.

[2.3] H. Schneider, J. Schreuer, B. Hildmann, Structure and properties of mullite-A review, Journal of the European Ceramic Society, 28 (2008) 329-344.

[2.4] V. Viswabaskaran, F. D. Gnanam, M. Balasubramanian, Mullitisation behaviour of calcined clay- alumina mixture, Ceramics International, 29 (2003) 561-571.

[2.5] N. L. Bowen and J. W. Greig, The system: Al_2O_3-SiO_2, J. Am. Ceram. Soc., 7 [4] (1924) 238- 254.

[2.6] E. C. Shears and W. A. Archibald, Aluminosilicate refractories, Iron Steel, 27 (1954) 26-30 and 61-65.

[2.7] S. Aramaki and R. Roy, Revised phase diagram for the system Al_2O_3-SiO_2, J. Am. Ceram. Soc., 45 [5] (1962) 229-42.

[2.8] I. A. Aksay and J. A. Pask, Stable and Metastable equilibria in the system SiO_2-Al_2O_3, Journal of the American Ceramic Society, 58 [11-12] (1975) 507-512.

[2.9] F. J. Klug, S. Prochazka, and R. H. Doremus, Alumina–silica phase diagram in the mullite region, J. Am. Ceram. Soc., 70 (1987) 750-759.

[2.10] D. J. Duval, S. H. Risbud and J. F. Shackelford, Structure, (J.F. Shackelford and R.H. Doremus (eds.), Ceramic and Glass Materials) Properties and Processing, Chapter-2 Mullite, Springer 2008.

[2.11] C. Y. Chen, G. S. Lan, and W. H. Tuan, Preparation of mullite by the reaction sintering of kaolinite and alumina, Journal of the European Ceramic Society, 20 (2000) 2519-2525.

[2.12] P. Kansal and R. M. Laine, A processable mullite precursor prepared by reacting silica and aluminium hydroxide with triethanolamine in ethylene glycol: structural evolution on pyrolysis, Journal of Am. Ceram. Soc., 80 [10] (1997) 2597-2606.

[2.13] R. Gopi Chandran and K. C. Patil, A rapid combustion process for the preparation of crystalline mullite powders, Materials Letters, 10 [6] (1990) 291-295.

[2.14] J. Temuujin, K. Okada, K. J. D. Mackenzie, Characterization of aluminosilicate (mullite) precursor preparrd by a mechnochemical process, J. Mater. Res., 13 [8] (1998) 2184-2189.

[2.15] J. Temuujin, K. Okada and K. J. D. Mackenzie, Formation of mullite from mechanochemically activated oxides and hydroxides, Journal of European Ceramic Society, 18 (1998) 831-835.

[2.16] L. S. Cividanes, T. M. B. Campos, L. A. Rodrigues, D. D. Brunelli, G. P. Thim, Review of mullite synthesis routes by sol-gel method, J. Sol-Gel Sci. Technol., 55 (2010) 111-125.

[2.17] I. Jaymes and A. Douy, Homogeneous precipitation of mullite precursors, Journal of Sol-Gel Science and Technology, 4 (1995) 7-13.

[2.18] J. Roy, N. Bandyopadhyay, S. Das, S. Maitra, Studies on the formation of mullite from diphasic Al_2O_3-SiO_2 Gel by fourier tranform infrared spectroscopy, Iran. J. Chem. Chem. Eng., 30 [1] (2011) 65-71.

[2.19] S. Sugita Sueyoshi and C. A. Contreras Soto, Fine pure mullite powder by Homogeneous precipitation, Journal of the European Ceramic Society, 18 (1998) 1145-1152.

[2.20] K. Okada and N. Otsuka, Characterization of the Spinel Phase from SiO_2-Al_2O_3 Xerogels and the Formation Process of Mullite, J. Am. Ceram. Soc., 69 [9] (1986) 652-656.

[2.21] J. S. Lee, S. C. Yu, Characteristics of mullite prepared from co-precitated $3Al_2O_3$-SiO_2 powder, Journal of Materials Science, 27 (1992) 5203-5208.

[2.22] N. M. Bobkova, I. V. Kavrus, E. V. Radion and F. Popovskaya, Formation of mullite obtained by coprecipitation, Glass and Ceramics, 55 [5-6] (1998) 186-188.

[2.23] A. K. Chakravorty, Effect of pH on 980 °C spinel phase-mullite formation of Al_2O_3-SiO_2 gels, Journal of materials science, 29 (1994) 1558-1568.

[2.24] G. M. Anil Kumar, P. Mukundan, A. D. Damodaran, K.G.K. Warrier, Effect of precursor pH on the formation characteristics of sol-gel mullite, Materials letters, 33 (1997) 117-122.

[2.25] J. E. Lee, J. W. Kim, Y. G. Jung, C. Y. Jo, U. Paik, Effect of precursor pH and sintering temperature on synthesizing and morphology of sol-gel processed mullite, Ceramics International, 28 (2002) 935-940.

[2.26] C. C. Osawa and C. A. Bertran, Mullite formation from mixtures of alumina and silica sols: Mechanism and pH effect, J. Braz. Chem. Soc., 16 [2] (2005) 251-258.

[2.27] S. H. Hong and G. L. Messing, Anisotropic grain growth in diphasic-gel-derived titania-doped mullite, J. Am. Ceram. Soc. 81 [5] (1998) 1269-1277.

[2.28] J. E. Lee, J. W. Kim, Y. G. Jung, U. Paik, Effect of precursor pH and composition on the grain morphology and size of mullite ceramics in aqueous system, Materials Letters, 57 (2003) 3239-3244.

[2.29] X. H. Jin, L. Gao, J. K. Guo, The structural change of diphasic mullite gel studied by XRD and IR spectrum analysis, Journal of European Ceramic Socity, 22 (2002) 1307-1311.

[2.30] K. Wang and M. D. Sacks, Mullite formation by endothermic reaction of alpha alumina/silica microcomposite particles, J. Am. Ceram. Soc., 79 [1] (1996) 12-16.

[2.31] A. L. Campos, N. T. Silva, F. C. L. Melo, M. A. S. Oliveira, G. P. Thim, Crystallization Kinetics of orthorrombic mullite from diphasic gels, Journal of Non-Crystalline Solids, 304 (2002) 19-24.

[2.32] H. J. Kleebe, F. Siegelin, T. Straubinger, G. Ziegler, Conversion of Al_2O_3-SiO_2 powder mixtures to 3:2 mullite following the stable or metastable phase diagram, Journal of the European Ceramic Society, 21 (2001) 2521-2533.

[2.33] S. Sundaresan and I. A. Aksay, Mullitization of diphasic aluminosilicate gels, J. Am. Ceram. Soc., 74 [10] (1991) 2388-2392.

[2.34] F. Kara and J. A. Little, Sintering behaviour of precursor mullite powders and resultant microstructures, Journal of the European Ceramic Society, 16 (1996) 627-635.

[2.35] P. D. D. Rodrigo and P. Boch, High purity mullite ceramics by reaction sintering, Int. J. High Technology Ceramics, 1 (1985) 3-30.

[2.36] T. Ebadzadeh, Formation of mullite from precursor powder: sintering, microstructure and mechanical properties, Materials Science and Engineering, A355 (2003) 56-61.

[2.37] D. Amutha rani, F.D. Gnanam, Low temperature pressureless sintering of sol-gel derived mullite, Materials Science and Engineering, A264 (1999) 254–261

[2.38] D. Amutha rani, D. Doni Jayaseelan, F.D. Gnanam, Densification behaviour and microstructure of gel-derived phase-pure mullite in the presence of sinter additives, Journal of European Ceramic Society, 21 (2001) 2253-2257.

[2.39] J. She, P. Mechnich, M. Schmucker, H. Schneider, Low-temperature reaction-sintering of mullite ceramics with an Y_2O_3 addition, Ceramics International, 27 (2001) 847-852.

[2.40] J. Roy, N. Bandyopadhyay, S. Das and S. Maitra, Effect of CoO on the formation of Mullite Ceramics from Diphasic Al_2O_3-SiO_2 Gel, Journal of Engineering Science and Technology Review, 3 [1] (2010) 136-141.

[2.41] S. H. Hong and G. L. Messing, Mullite transformation kinetics in P_2O_5, TiO_2 and B_2O_3-doped aluminosilicate gels, J. Am. Ceram. Soc., 80 [6] (1997) 1551-1559.

[2.42] E. R. De Sola, F. Estevan, J. Alarcon, Low-temperature Ti-containing 3:2 and 2:1 mullite nanocrystals from single-phase gels, Journal of the European ceramic society, 27 (2007) 2655-2663.

[2.43] S. M. Naga, A. El-Maghraby, Preparation and characterization of porous fibrous mullite bodies doped with TiO_2, Materials characterization, 62 (2011) 174-180.

[2.44] S. Maitra, J. Roy, Effect of TiO_2 and V_2O_5 additives on chemical mullite, Advances in ceramic science and engineering, 2 [3] (2013) 130-133.

CHAPTER 3

EXPERIMENTAL WORK

3.1 Materials

Aluminium nitrate nonahydrate of purity 99% (E-Merck, India) and fumed silica (Cab-O-Sil) were used as source materials for alumina and silica respectively. 25% NH_3 (Ammonia solution, analytical grade) was used as the precipitant. TiO_2 (Fisher Scientific) was used as sintering additive, and PVA (Polyvinyl alcohol) was used as a binder.

3.2 Methods

3.2.1 Synthesis of powder precursor:-

Preparation of Aluminium nitrate Solution:-

The stock solution of aluminium nitrate was prepared by dissolving 240 gm. of $Al(NO_3)_3.9H_2O$ in 150 ml. of distilled water. The solution was luke warmed and stirred for proper mixing of solid aluminium nitrate. 10 ml of this salt solution was taken in a crucible, slowly dried and finally calcined at a temperature of 1100 °C. From the difference of weight of the empty crucible and the crucible containing calcined mass, the amount of alumina present in the solution was calculated. The result was given in table 3.1.

Table 3.1 Determination of alumina in aluminium nitrate solution.

Volume of aluminium nitrate solution taken (ml)	**Weight of empty crucible W_1 (g).**	**Weight of crucible with sample after firing W_2 (g).**	**Weight of fired mass W_2-W_1 (g).**	**Strength of solution (g/cc)**
5	80.157	80.540	0.383	0.0766 gm./ml.

Chemical analysis of fume silica:-

The amount of silica present in fumed silica sample was estimated by hydrofluoric acid treatment method. The result is given in table 3.2.

Table 3.2 Determination of silica present in fume silica.

Weight of empty platinum crucible W_1 (g)	**Weight of empty platinum crucible with sample W_2 (g)**	**Weight of crucible with sample after heating W_3 (g)**	**Amount of silica present (% Wt)**
24.1127	24.2649	24.1147	98.67

Batch preparation

Total seven batches of mullite powder precursor are prepared of which three batches (A, B and C) are of the same composition, but the pH of the solution during precipitation is varied from 6–10. Another four batches (B-1, B-2, B-3, and B-4) are prepared by varying the amount of sintering additive titania in the range 1.5 to 6 wt%. The detail process is given in the form of flow sheet-1, and the batch compositions are given in table 3.3.

Table 3.3 Batch compositions.

Batch	**pH**	**Al_2O_3 wt %**	**SiO_2 wt %**	**TiO_2 wt %**
Batch A	6	72	28	0
Batch B	8	72	28	0
Batch C	10	72	28	0
Batch B-1	8	70.92	27.58	1.5
Batch B-2	8	69.84	27.16	3
Batch B-3	8	68.76	26.74	4.5
Batch B-4	8	67.68	26.32	6

The required amounts of raw materials for 100 gm of prepared precursor powder are described in the table 3.4.

Table-3.4 Batch calculations.

Batch	Aluminium Nitrate solution (ml)	Fume Silica (gm.)	TiO_2 (gm.)
Batch A	939.947	28.3722	0
Batch B	939.947	28.3722	0
Batch C	939.947	28.3722	0
Batch B-1	926.240	27.9489	1.5
Batch B-2	911.749	27.5229	3
Batch B-3	897.650	27.0972	4.5
Batch B-4	883.550	26.6619	6

Process

Mullite precursor powder was synthesized by mixing aluminium nitrate solution and fumed silica solution in such a proportion that it maintains Al_2O_3:SiO_2 molar ratio as 3:2 in the final product. The slurry was mixed properly by stirring the mixture for one hr at 50 °C. The pH of the slurry was found to be around 2. Then chemical precipitation was done by reverse strike using ammonia as precipitating agent. During precipitation, pH was varied in the range 6-10 to study the effect of the pH change on the properties of the prepared mullite precursor powder. The formed gel-like mass was equilibrated for 24 h to complete the precipitation reactions. Then the extraneous soluble impurities were removed by washing the gel several times with warm water. The solid mass left was dried at 110±10 °C for 12 hrs. The dried mass was powdered using agate mortar pestle.

Different characterization techniques like DSC-TG, XRD, FTIR, FESEM, Particle size analysis, Surface area analysis, Dilatometer study, etc. were carried out, and it was found that the precursor powder formed at pH-8 exhibited better properties. Therefore, the sintering

study of the precursor powder is continued with that powder only. In this process, TiO_2 is used as a sintering additive, and it is mixed in the solution after proper mixing of aluminium nitrate and fume silica. This solution was stirred for 1-2 hrs. TiO_2 is mixed in the range of 1.5 - 6 weight % and the pH was maintained around 8. The detail synthesis process is represented by the following flow sheet-1.

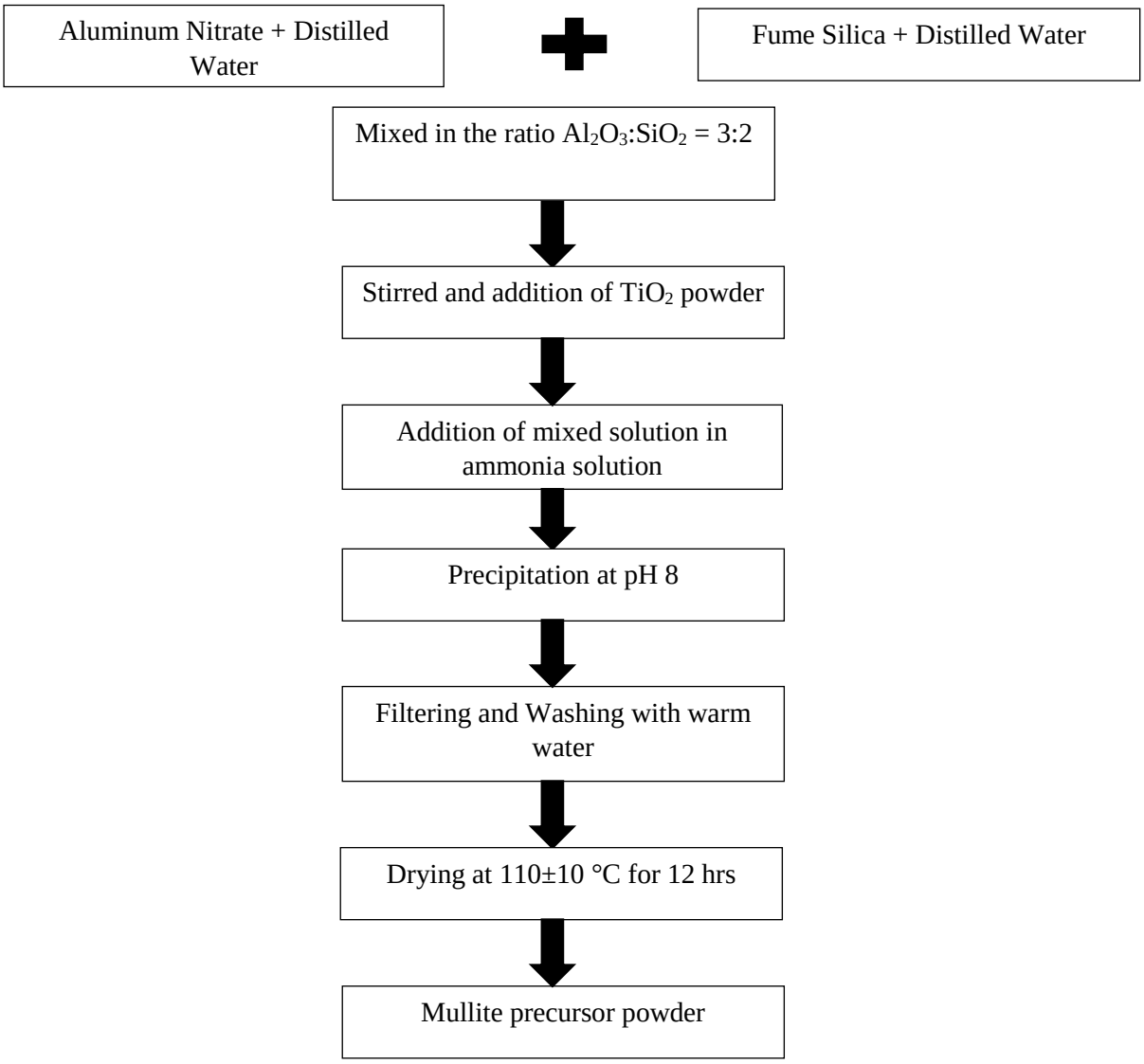

Flowchart-1 Synthesis process of Mullite powder precursor.

3.2.2 Sintering of powder precursor:-

The fine dried precursor powder is calcined at 900 °C for one hour to avoid excessive shrinkage during firing. Then 80% calcined powder and 20% uncalcined powder was mixed with 3% PVA solution to form the final pellets, where, PVA acts as a binder for shape formation. Compacts of 12.5 mm diameter and 5 mm thickness are prepared by uniaxial pressing at 240 MPa pressure for a holding period of 90 sec using 0.5 gm of powder. Samples are then dried at 110 °C. Before firing, the green dimensions of the pellets are measured. The dried samples are then fired at three different temperatures 1450 °C, 1550 °C and 1650 °C for a soaking period of 2 h in each case. An electrically operated laboratory furnace is used for this purpose using an on/off control system. A constant heating rate of 3 °C /min up to 500 °C followed by 60 minutes soaking and 5 °C/min up to the required maximum temperature followed by 120 minutes soaking was maintained in each firing. The detail sintering process is represented by the following flow sheet-2.

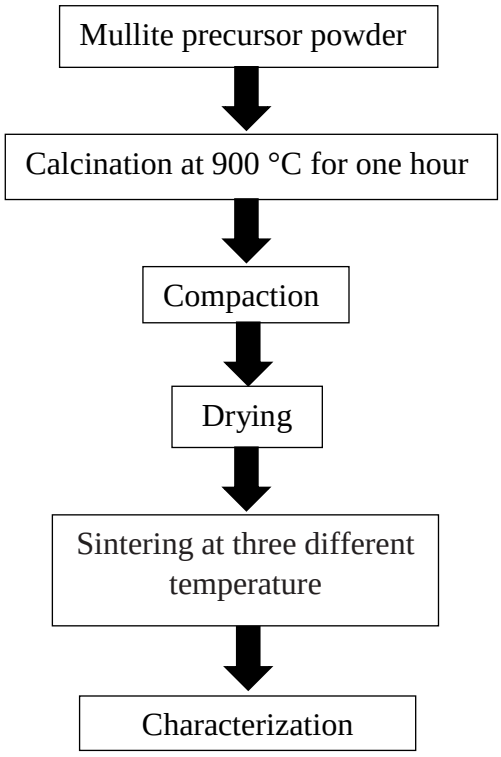

Flowchart-2 Sintering process of Mullite powder precursor.

3.3 Methodology:-

Different characterization techniques like DSC-TG, XRD, FTIR, FESEM, Particle size analysis, Surface area analysis, Dilatometer study, etc. were carried out to characterize the prepared mullite precursor powder. Sintered pellets were characterized by Bulk density, Apparent porosity, Shrinkage, Flexural strength, XRD, FTIR, FESEM study, etc.

3.3.1 DSC-TG analysis

The thermal analysis was done to study the decomposition and crystallization behaviour of the precursor powder. The analysis was carried out up to a temperature 1400 °C at a rate of 10 °C/min in an inert atmosphere. The dried precursor powder was characterized by using NETZSCH STA Germany (model no. 449C/4/MFC/G).

3.3.2 Phase identification (XRD analysis)

The X- Ray Diffraction study was done to investigate the different phases present in the samples. The X-ray diffraction was carried out by RIGAKU JAPAN/ ULTIMA-IV using Cu Kα radiation. The data obtained was analysed with the help of Philips X- Pert High Score software, and the peaks were identified. The scanning range of 2θ was taken from 20° to 80° with a scanning speed of 20°/min and accelerating voltage of 30 KV. By using X-ray diffraction technique, other relevant information like crystal structure, the crystallinity of the material, crystallite size, strain, etc. were also be identified.

3.3.3 FTIR analysis

FTIR analysis was carried out by using FTIR spectrometer (Perkin Elmer, SQ 300S) in a wavelength range 400-4000 cm^{-1}. It provides information about the functional groups and the type of bonds present. The sample was mixed with KBr in a ratio of 1:12 (sample to KBr).

The mixture was ground by using agate mortar to make a fine powder. The prepared powder was compacted to make a pellet at a pressure of 1 tons for 1 min.

3.3.4 Microstructure analysis (FESEM)

Microstructure analysis was done using Field Emission Scanning Electron Microscope (Nova Nano SEM/ FEI 450). The images of fine powder samples and fracture surface of pellets were taken at different magnification. Platinum coating was applied on the sample surface to make it conducting.

3.3.5 Particle-size analysis

Particle size analysis was carried out by a laser diffraction method with multiple scattering technique using Zeta-sizers-Particle size analyzer (Malvern/Nano ZS). The relation between particle size and the scattering angle is such that the large particles scatter at low angles while small particles scatter at high angles. The light scattering depends upon the refractive index of powder as well as the refractive index of dispersant and medium. This instrument combines a particle size analyzer and a zeta potential analyzer for particles, ranging from nanometer to several micrometer. The prepared precursor and 800 °C calcined powder samples were dispersed in water using horn type ultrasonic processor [Ultrasonic Processor Sonopros, PR1000 MP]. Then the experiment was carried out in a computer controlled particle size analyzer to find out the particles size distribution.

3.3.6 Surface area analysis

The surface area was analysed by using BET (Brunauer, Emmet and Teller) surface-area and pore size analyser (Quantachrome/ AUTOSORB-1). The instrument measures the surface area > 0.05 m^2/g with a max degassing temperature of 350 °C. The technique for evaluating surface area of a porous material relies on the process of adsorption and desorption of a non-reactive gas (e.g. N_2 or He) on the surface of a material.

The average particle size d_{BET} was calculated by assuming all the particles to have same spherical shape and size. The average particle diameter (D) is calculated by using following formula,

$$\boldsymbol{D = \frac{6}{\rho s}}$$

Where D= average particle diameter, ρ= true density of material (gm/cm^3), s= specific surface area.

3.3.7 Dilatometer study

The linear expansion or shrinkage was measured by using Dilatometer (Netzsch, Germany, DIL 402C) up to a temperature 1400 °C using a heating rate of 10 °C/min and the sample size is 11×3×3 mm. The dilatometer is a thermo-analytical technique for measuring expansion or shrinkage of a material when subjected to a controlled temperature vs. time program.

3.3.8 Compaction of powder

The compaction of homogeneous powder into pellets was done by using an automatic hydraulic press (Model 3887, Carver Inc. USA). The circular die-punch was used for shaping the pellets. The weighed amount of powder was taken in a die and accurately levelled. Compacts of 12.5 mm diameter and 5 mm thickness were prepared by uniaxial pressing at 240 MPa pressure for a holding period of 90 sec.

3.3.9 Green Density measurement

Green density is the ratio of mass of the green body to its volume. It can be calculated by using following formula,

Green density = mass / volume.

Where, volume= $\pi r^2 h$, r = radius of pellet, h = height of pellet.

3.3.10 Sintering

The pressureless sintering of green pellets was carried out by using high-temperature electric furnace (Bysakh & Co. Kolkata) with on/off control system. Green pellets were sintered at three different temperatures 1450, 1550, 1650 °C for a soaking period of 2 h in each case. A constant heating rate of 3 °C /min up to 500 °C for 60 minutes was used to remove the binders. After that, the heating was continued at a rate of 5 °C / min up to the required sintering temperature with 120 minutes soaking time.

3.3.11 Percentage Linear Shrinkage and Percentage Volume Shrinkage measurement

The dimensions of green samples and sintered samples were measured with the help of Vernier Caliper. The percentage linear shrinkage was calculated by using the following formula.

$$\textit{Percentage Linear Shrinkage} = ((\textit{Initial length} - \textit{Final length}) / \textit{Initial length}) \times 100.$$

Volume shrinkage was calculated by using formula,

$$\textit{Percentage Volume Shrinkage} = ((\textit{Initial Volume} - \textit{Final Volume}) / \textit{Initial Volume}) \times 100.$$

3.3.12 Bulk Density and Apparent Porosity measurement

Bulk density and Apparent porosity of a sintered pellet were calculated by using Archimedes principle. In this method, pellets were immersed in kerosene which was kept it in vacuum desiccators for 45 min to fill the open pores with kerosene completely. Bulk density was calculated by using the following formula,

$$\textit{Bulk density} = (\textit{Dry weight} / \textit{Soaked weight} - \textit{Suspended weight}) \times \rho\ (g/cm^3).$$

Where ρ= density of the medium, here medium was Kerosene=0.81gm/cm^3.

Apparent Porosity was calculated by using formula,

Apparent porosity= (soaked weight- dry weight) / (soaked weight- suspended weight).

3.3.13 Flexural Strength measurement

It is defined as the ability of a material to resist deformation under load. It is also known as modulus of rupture, fracture strength or bend strength. It was measured by using Three-Point Bend test which is performed on a universal testing machine (TINIUS OLSEN H10K-S UTM). For this test, a rectangular bar of dimension 50×10×10 mm was used. Flexural strength can be calculated by using following formula,

$$\boldsymbol{\sigma = \frac{3PL}{2WD^2}}$$

Where, σ = the maximum stress, P = the fracture load, L = span length, W = width and d= breadth of the specimen. The unit of flexural strength is- MPa or N/m^2.

CHAPTER 4

RESULTS AND DISCUSSIONS

4. Results and Discussions:

4.1 Processing and characterization of diphasic mullite precursor powder

Mullite precursor powder was synthesized at three different pH conditions as described in the experimental section. The characterization part of those prepared powder is discussed here.

4.1.1 Thermal analysis of precursor powder

The thermogravimetric curves of the precursor powder of batch-A and B are shown in figure 4.1.1. The thermal analysis curves for batch B and C are similar so, the curves for batch-C is not shown here. From the figure, it is clear that the weight loss in all the batches is almost same (~27%) except for batch A, where the weight loss is higher around 33% and completed at 700 °C. In case of batch B and C though the weight loss is less compared to batch A, but it continued up to higher temperature 900 °C. All the powder samples show three stages weight losses. The weight losses and the corresponding endothermic peaks shown in the DSC curves (figure 4.1.1) are due to the loss of moisture, dehydration of silicic acid gel and dehydration and dehydroxylation of alumina hydroxide gel.

At the higher temperature range a wide exothermic hump in the temperature range 800-1000 °C is attributed to Al-Si spinel / γ Al_2O_3 formation. In lower pH sample, a weak exothermic peak at 1090 °C probably indicates the transformation of this γ Al_2O_3 to other transition phase alumina. At further higher temperature mullite phase is expected to be form as a result of the reaction between these transition alumina phases with free silica. In higher pH samples, the two overlapping exothermic peaks in the temperature range 1200 °C - 1300 °C indicate two step mullite crystallization reactions. In case of diphasic precursor powder, sometimes on calcinations, segregation of alumina rich and silica-rich regions are formed. The alumina rich region at higher temperature converted to mullite through the transformation of Al-Si spinel phase [4.1]. The first peak is assumed to be responsible for this phenomenon. The second

peak is due to the mullite formation by the reaction between transient alumina and silica-rich amorphous phase.

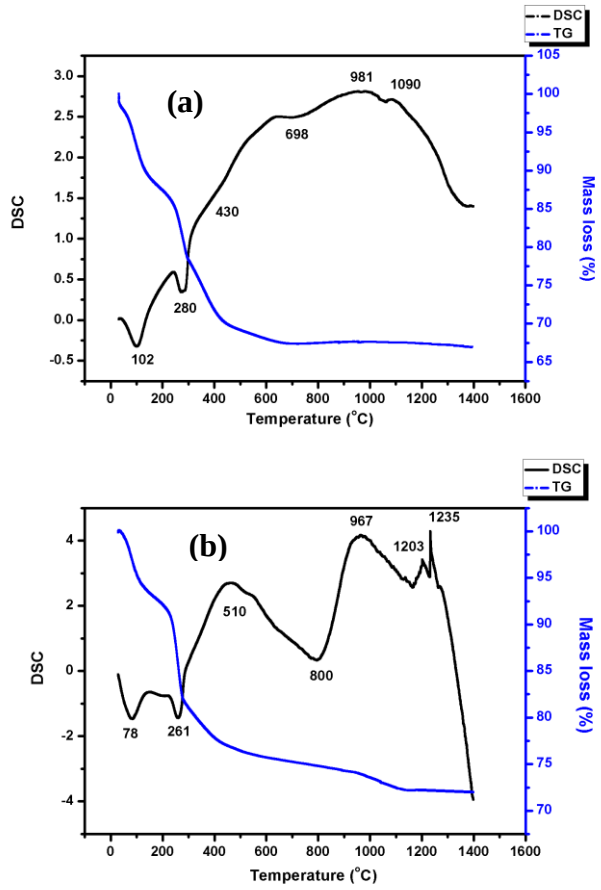

Figure 4.1.1 TG-DSC curve for (a) Batch A, (b) Batch B.

According to TG-DSC results there is no difference between the powder precursor of batch B and C. Fume silica when dispersed in an aqueous medium, it initially forms a stable sol. Here water molecules form H-bond with silanol group (Si-OH) present on the silica surface. It generates a solvation layer that coats each silica particle. The firm bonding of these water molecules within this solvation layer is then expected to produce a short range repulsive force preventing particle coagulation as shown in figure-4.1.2 [4.2, 4.3].

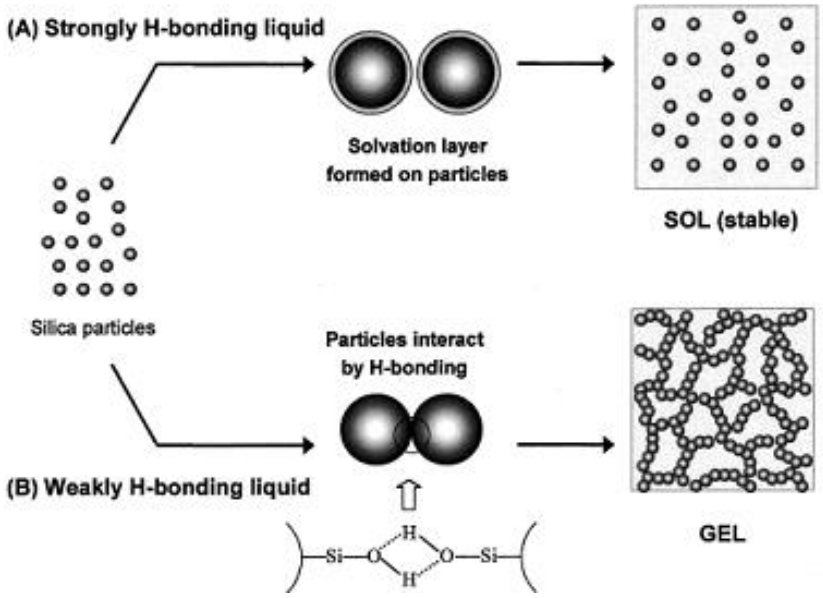

Figure 4.1.2 Silica sol and silica gel formation [4.4].

When this is mixed with the aluminium nitrate solution, then the solution became acidic, the pH value is around 2. At this pH, the surface of the silica particle is positively charged. When this solution is mixed with ammonium hydroxide, the pH rises, and the formation of aluminium hydroxide gel and polysilicic acid occurs. Thus, the formed gel is diphasic in nature. At high pH above pH 7 up to 10, silica dissolves as silicates. The hydrous silica particles are now negatively charged. So they repel each other, and there is no polymerization of hydrolyzed silica and evolution of water [4.5]. This phenomenon is probably related to the lower amount of weight loss for the powder prepared at higher pH. Here though the weight loss is less around 27%, but it continued up to the higher temperature around 900 °C. At higher pH around 8-10 due to condensation of Al^{3+} ion through olation and oxolation mechanism a polynuclear hydroxide formed [4.6, 4.7].

$[M(H_2O)_6]^{3+} \leftrightarrow [M(H_2O)_5OH]^{2+} + H^{+}$…….(1)

$[(H_2O)_5M{-}OH{-}M(H_2O)_5]^{5+}$…….(2)

Because of this polycondensation, particle size is bigger at higher pH. In the acidic condition, the equilibrium of equation-(1) shifted towards left thus inhibit poly-condensation. Therefore, the delayed weight loss in the diphasic gel formed at higher pH may be due to the trapping of water molecule within this large polymer [4.8].

4.1.2 Phase identification (XRD analysis)

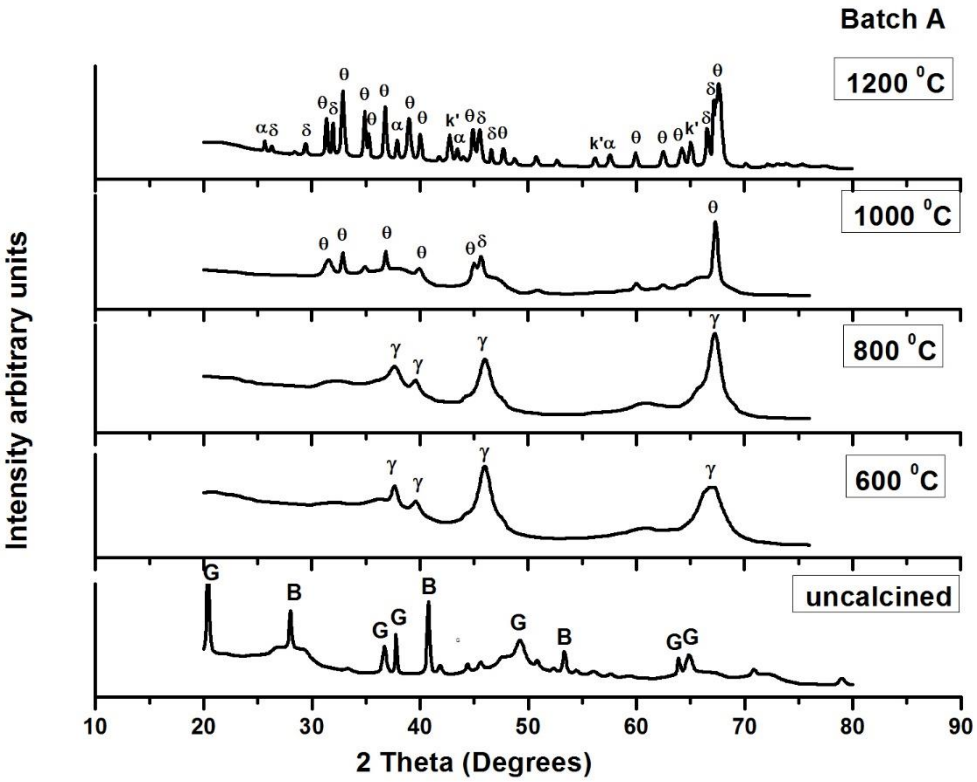

Figure 4.1.3 XRD patterns of Batch-A (G-Gibbsite; B-Bayerite; γ-Gamma Alumina; δ-Delta Alumina; θ-Theta Alumina; α-Alpha Alumina; κ'- Kappa Alumina).

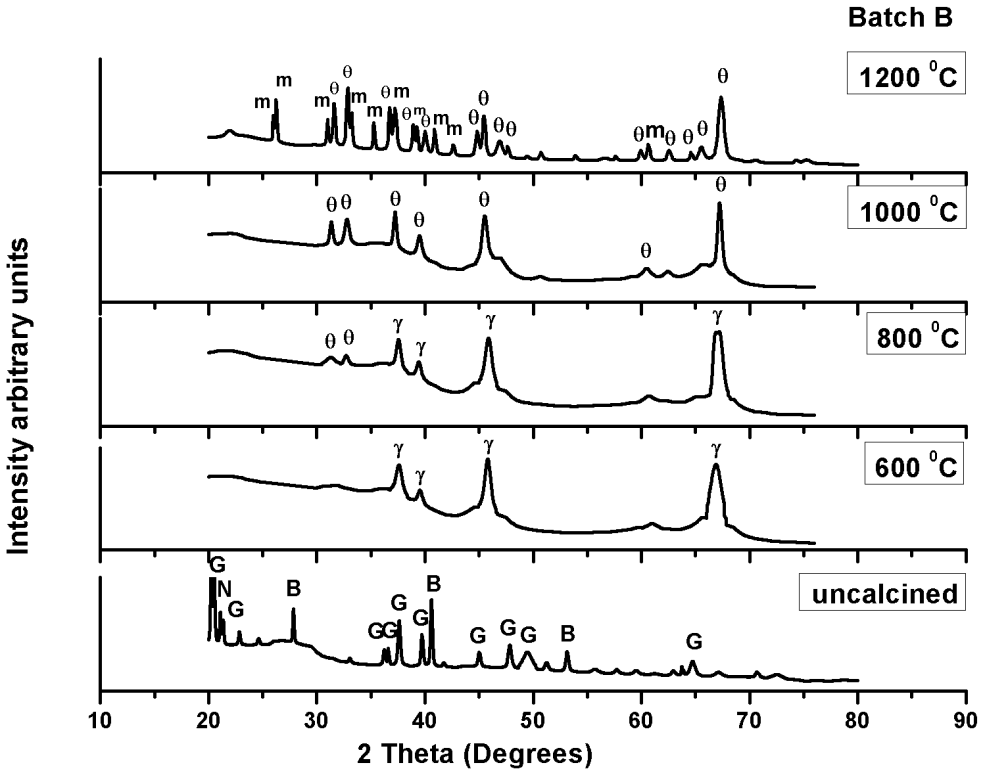

Figure-4.1.4 XRD patterns of Batch-B (G-Gibbsite; B-Bayerite; γ-Gamma Alumina; δ-Delta Alumina; θ-Theta Alumina; m-Mullite).

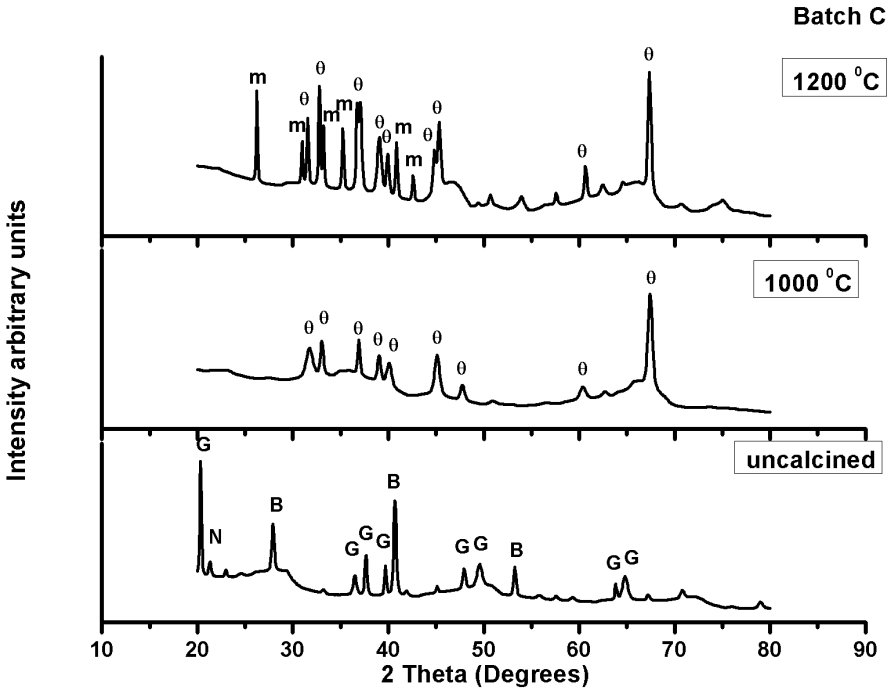

Figure-4.1.5 XRD patterns of Batch-C (G-Gibbsite; B-Bayerite; γ-Gamma Alumina; δ-Delta Alumina; θ-Theta Alumina; m-Mullite).

The X-ray diffraction study of mullite precursor powder prepared at pH-6, pH-8 and pH-10 has been done, and the corresponding diffraction pattern of uncalcined powder samples and calcined powder samples (calcined at different temperatures) are shown in figure 4.1.3, 4.1.4 and 4.1.5 respectively. From the patterns, it is clear that Bayerite and Gibbsite are the two distinct phases that are present in the powder precursor prepared at different pH. After calcining at 600 °C the gel transform to a mixture of an amorphous phase and γ-alumina. Further heating leads to the formation of other transition phase alumina like δ-alumina and θ alumina though silica still remains amorphous. At 1200 °C, batch-B exhibits mullite phase but for batch-A, there is no mullite phase formation though some new transition alumina phases and the stable α-alumina phase is found to form. The X-ray diffraction pattern of precursor powder and calcined powder prepared at pH-8 and pH-10 are similar. The main differences for the calcined powder prepared at pH-6 and pH-8 are the appearance of transition alumina phases at comparatively lower temperature in case of higher pH sample, and the formation of higher amount of mullite phase at 1200 °C for the same sample.

The presence of transition alumina phases at 1200 °C is quite unusual but not impossible. Particularly in stoichiometric composition the coexistence of amorphous silica, metastable alumina and mullite is already reported [4.1, 4.9, 4.10]. Only in alumina rich composition above 1200 °C, θ alumina decomposed and converted to mullite and corundum [4.11]. Many researchers showed the presence of amorphous silica stabilized transition alumina phases in mullite precursor powder at and around 1200 °C [4.12, 4.13]. It is already established that the apparent stability domain of transition aluminas are enlarged by the addition of silica [4.14]. In the presence of fumed silica, if γ-alumina is heat treated at 1200 °C then θ alumina, and other transition alumina phases are formed. In the absence of fumed silica, at the same temperature α alumina is the main product [4.15]. The mechanism of retarding alumina phase transition is considered as follows. In this diphasic powder during thermal treatment as the

transition alumina phases formed then the amorphous silica forms a coating on the surface of the γ-alumina particle and prevents particle contact. This phenomenon helps to suppress the coagulation of γ-alumina particle and in turn retard phase transition [4.15].

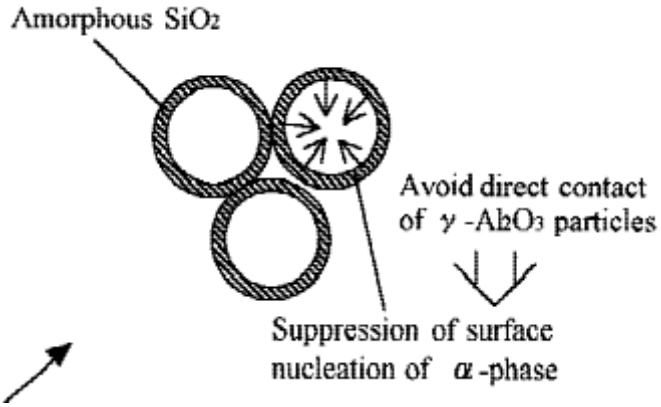

Figure 4.1.6 Schematic representation of amorphous silica stabilised transition alumina [4.15].

In the DSC curve, the broad exothermic peak above 900 °C which is indicated either for Al-Si spinel formation or for γ alumina formation appears from the XRD study as the γ alumina phase. Actually the Al-Si spinel, which is a solid solution of γ alumina and silica, is very difficult to distinguish from γ alumina phase. The presence of two overlapping exothermic peak in the DSC trace for mullite powder prepared at higher pH in the temperature range 1200 °C-1300 °C supports the presence of Al-Si spinel phase along with γ alumina phase. Many authors showed that [4.16-4.18] spinel phase contained a certain quantity of silica incorporated in γ alumina, so it easily converted to mullite phase around 1200 °C. The pure γ alumina phase at higher temperature converted to other transition alumina phase and subsequently reacts with the amorphous silica to form mullite. This two-step mullite formation may be one of the reasons for the presence of higher amount of mullite in pH-8 sample calcined at 1200 °C.

In a diphasic precursor, mullite formation occurs mainly by the reaction between transition alumina and amorphous silica [4.19]. Here at higher pH aluminium hydrogel preferentially flocculates and gets converted to different transition alumina form early, which facilitates the silica-transition alumina reaction for mullite formation, another thing is that at higher pH, above pH-7, silica particle are negatively charged particle, they repel each other and is easily available for reaction with transition alumina to form mullite.

4.1.3 FTIR analysis

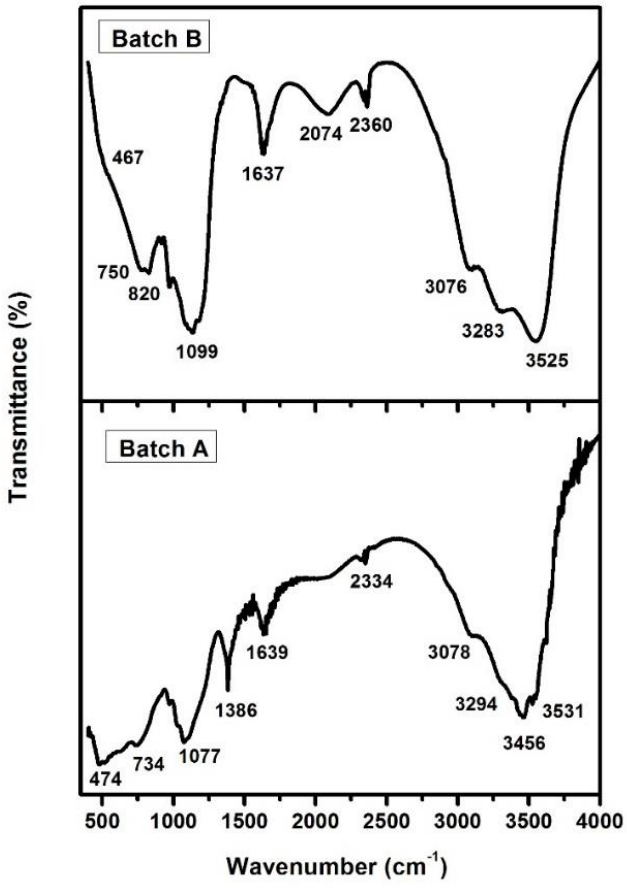

Figure 4.1.7 FTIR spectra of batch-A and B precursor powder.

Figure 4.1.7 shows the FTIR spectra of mullite precursor powder prepared at pH-6 and pH 8. The wide and strong absorption band in the range 3000 cm^{-1} - 3600 cm^{-1} in both cases, indicates stretching region of OH group and H_2O molecule. The deconvolution of this absorption region reveals four different bands due to bridging H_2O, bridging OH groups and non-bridging H_2O, non-bridging OH groups. The absorption band around 3531 cm^{-1} and 3456 cm^{-1} represent stretching mode of OH group and H_2O molecule respectively without any hydrogen bridging. On the other hand, the OH stretching mode around 3294 cm^{-1} and H_2O stretching mode around 3078 cm^{-1} requires strong hydrogen bonding. A similar type of water and hydroxide bridging is also found in the glass structure [4.20, 4.21]. During heat treatment, hydrogen-bonded molecular water and hydroxide groups eliminated comparatively easily and a minor amount of non-bridging OH group and water molecules still remains at a higher temperature. In heat treated powders, the presence of band around 3440 cm^{-1} supports this interpretation. Thermal treatment of the precursor powder causes dehydration and dehydroxylation along with strong and discontinuous condensation. This condensation produces a large number of closed micro pores that trapped a portion of the water molecule [4.21]. This phenomenon is responsible for the presence of the water molecule in calcined powder.

The absorption band around 1639 cm^{-1} and 1386 cm^{-1} is due to bending moment of water molecule and presence of nitrate group [4.20]. The presence of absorption band around 820 cm^{-1} and 1077 cm^{-1} are assigned to the Si-OH stretching mode and bending mode. The stretching mode of Al-O-Al linkage and Si-O-Si linkage of the gel network are observed around 734 cm^{-1} and 474 cm^{-1} [4.22]. Thus, there is a clear indication of the presence of Al-O-Al linkage and Si-O-Si linkage in the precursor powder. The absence of Si-O-Al linkage in the same powder implies the inhomogeneity and diphasic nature of the powder precursor.

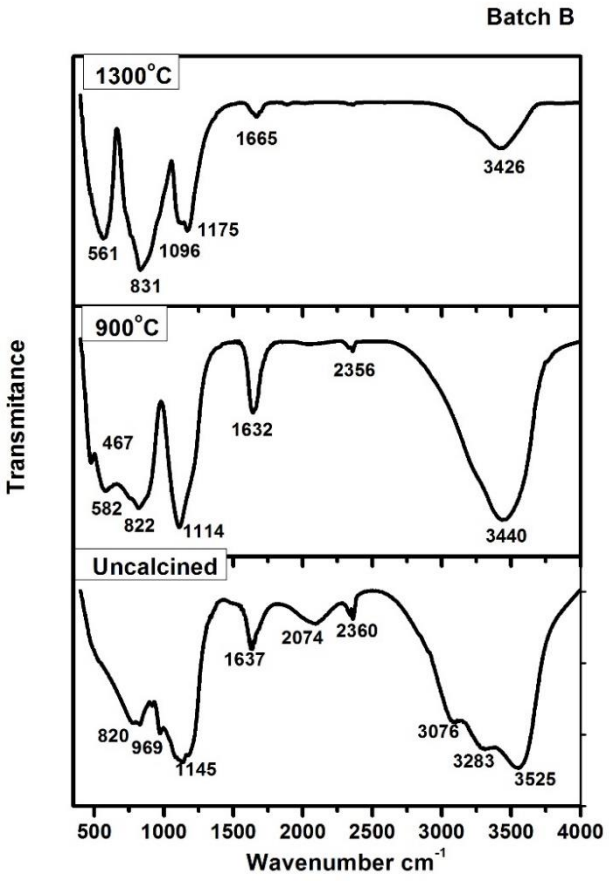

Figure 4.1.8 FTIR spectra of batch- B (precursor powder and calcined powder).

FTIR spectra of powder prepared at pH-8 and calcined at 900 °C and 1300 °C is shown in Fig 4.1.8. The structural change occurring in the powder precursor during thermal treatment is recorded by this infrared analysis. As the calcination temperature raises, the band corresponding to the stretching and bending of water molecule becomes weaker. In 900 °C calcined powder the presence of Si-O stretching band at 1114 cm^{-1} and the band corresponding to the Si-O bending mode at 467 cm^{-1} proves the presence of pure quality amorphous silica in this temperature range. Later, mullite forms by the reaction between amorphous silica and transition alumina causing shifting of Si-O band to the higher wave number. Finally, 1300 °C calcined powder shows absorption bands at 1096 and 1175 cm^{-1}. These bands are assigned respectively to the asymmetric stretching vibration of Si-O-Al and Si-O-Si network. This shifting of Si-O-Si asymmetric stretching frequencies to higher wave

numbers indicates the formation of mullite [4.20]. The absorption band at 820, 822 and 831 cm^{-1} in the powder precursor, 900 °C calcined powder and 1300 °C calcined powder are due to Al^{IV}-O stretching (tetra coordinated Al). The Al^{VI}-O stretching (hexacoordinated Al) is represented by the band at 582 and 561 cm^{-1} in 900 °C and 1300 °C calcined powder respectively [4.22]. The absence of Al^{VI}-O stretching band in the precursor powder shows the unavailability of the hexacoordinated aluminium ion. With increasing temperature, the Al^{IV}-O band expands and evolves into two bands at 900 °C, which become more prominent at 1300 °C.

4.1.4 Morphology study

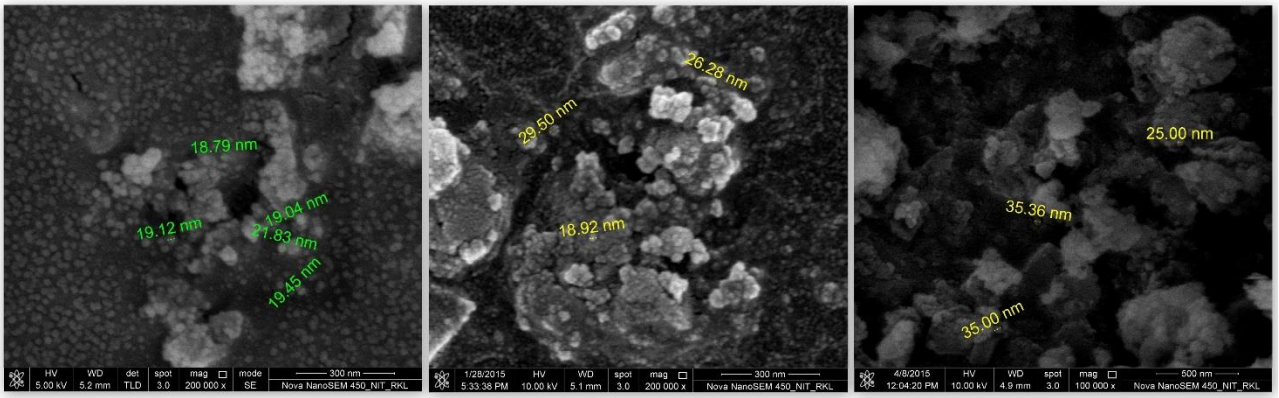

Figure 4.1.9 FESEM micrograph of batch A, B and C powder precursor.

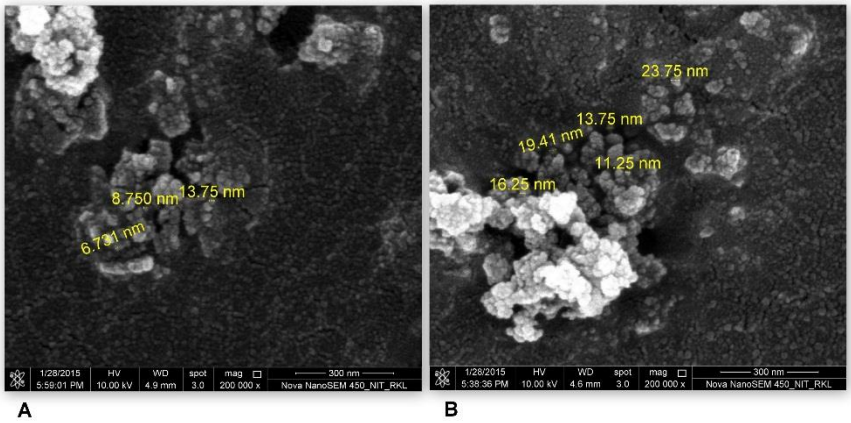

Figure 4.1.10 FESEM micrograph of batch A and B calcined powder.

Figure 4.1.9 A, B and C shows, the FESEM micrograph of the precursor powder prepared at pH-6, pH-8 and pH-10 respectively. From the micrograph, it is clear that the powder is in agglomerated state and contains a dense aggregate of the primary particle. The size of the agglomerates and primary particles are finer for the powder prepared at lower pH. Actually the morphology of the prepared precursor powder is affected very much by the solution pH condition. In the basic condition, pH ≥ 8 there is a tendency to flocculation and formation of larger primary particle [4.23]. The powder morphology is modified slightly with calcination, as shown in figure 4.1.10, A and B of the calcined powder prepared at pH-6 and ph-8 respectively. The diffused pattern of agglomerates gets finer after milling of the calcined powder and the large aggregates are broken down into a smaller aggregate of nano-sized primary particle [4.20].

4.1.5 Dilatometer study

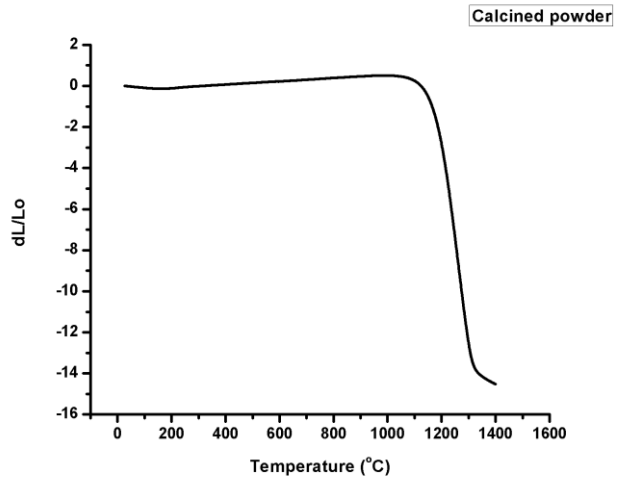

Figure 4.1.11 Dilatometric graph of batch B.

Figure 4.1.11 shows, the dilatometric study of batch B in the temperature range room temperature to 1400 °C. From the graph, it is observed that the sample size remains almost constant up to around 1100 °C. Above 1100 °C shrinkage occurs. The shrinkage is due to initiation of densification.

4.1.6 Surface area analysis

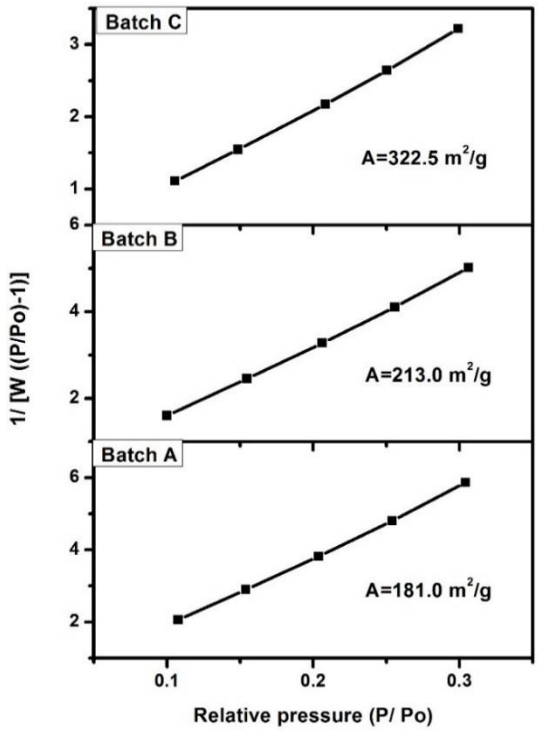

Figure 4.1.12 BET surface area plot of batch A, B and C.

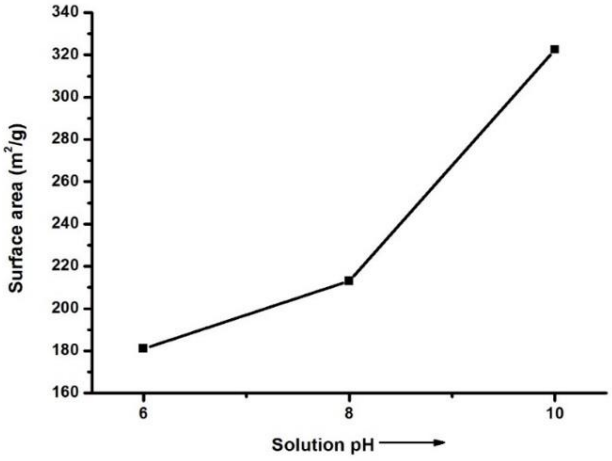

Figure 4.1.13 Plots of surface area vs. precipitation pH for precursor powders.

The BET surface area plots of different batches are shown in figure 4.1.12. The influence of solution pH on surface area of prepared mullite precursor powder is shown in figure 4.1.13. The surface area of the prepared powder is found to increase here with increasing pH of the solution. Generally at lower pH the process of hydrolysis and condensation is selective and controlled, that produces a linear polymer. At higher pH, greater than pH-7 due to the presence of a larger amount of OH ions, the hydrolysis and condensation are uncontrolled, and highly branched polymer forms. Therefore, it is expected that at higher pH, the particle size should be larger, and surface area should be lower, but, here we get the reverse trend. The change of solution pH affects both the primary particle size and agglomeration of the powder. At lower pH, the surface charge is positive and at higher pH the surface charge is negative for alumina gel in mullite precursor powder. At higher pH, due to the negative surface charge the repulsion between the particles is high, so the agglomeration is less. At intermediate pH around 6-7 particles have little surface charge and particles stick to one another to form agglomerates. This agglomeration causes a reduction of surface area in batch-A [4.24].

4.1.7 Particle size analysis

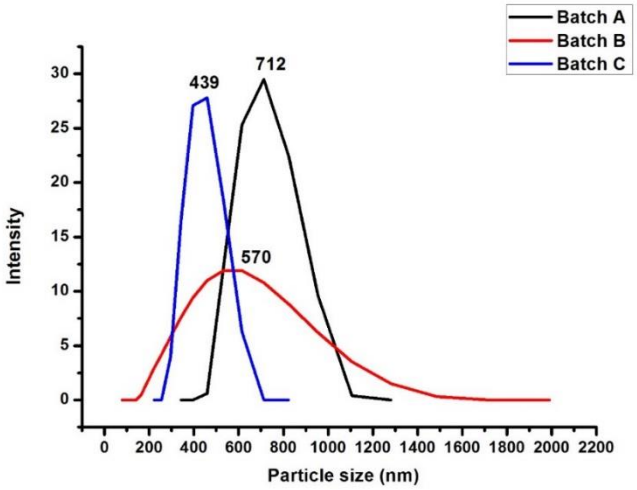

Figure 4.1.14 Particle size distribution of batch A, B and C powder.

Particle size distribution of the prepared mullite precursor powder of different batches is shown in figure 4.1.14. From the figure, it is found that the size distribution is mono-modal with the average particle size 712 nm, 570 nm and 430 nm for the batch A, B and C respectively. The observed particle size is much higher than the size found from the micrograph. This deviation is due to agglomerate formation. The larger agglomerate size for batch-A sample supports the result of lower surface area for the same.

4.2 Characterization of diphasic mullite precursor powder in presence of titanium oxide additive:

4.2.1 Thermal analysis of precursor powder

The use of titanium dioxide as a nucleating agent for the development of crystalline phases by controlled heat treatment of precursor powder is a well-known fact [4.25, 4.26]. Effect of titanium dioxide on the preparation and reaction sequence of monophasic mullite gel is already reported [4.27]. In this section the role of titanium oxide on phase formation, densification and microstructure of diphasic precursor powder is discussed.

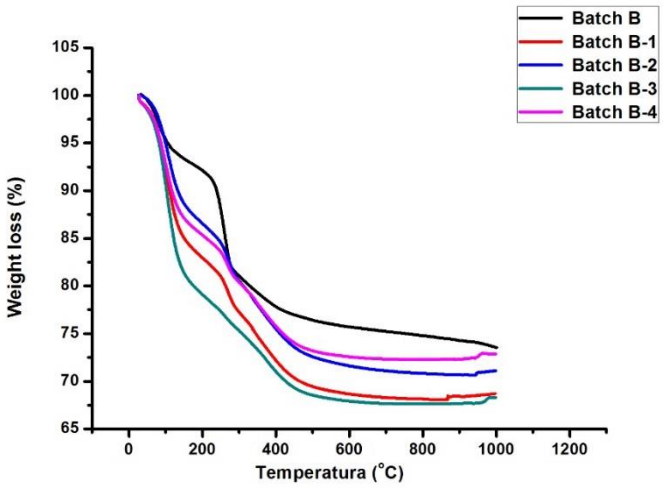

Figure 4.2.1 TG curve for Batch B, B-1, B-2, B-3 and B-4.

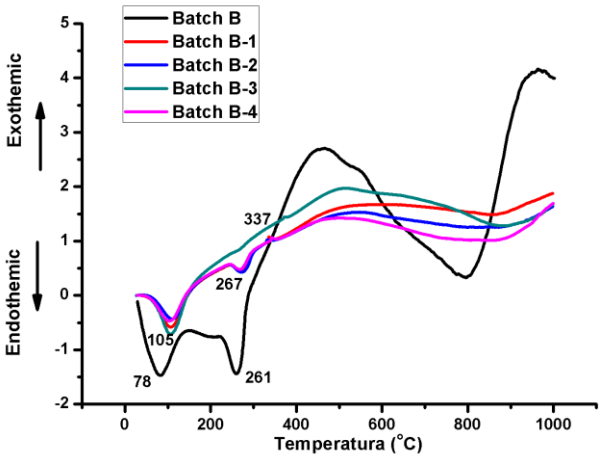

Figure 4.2.2 DSC curve for Batch B, B-1, B-2, B-3 and B-4.

Figure-4.2.1 and 4.2.2 show the TG and DSC plots of mullite powder precursor containing different wt% of TiO_2 additive. It is found from the figures that in presence of TiO_2 the % wt loss increases and the loss occurs in two stages. Up to 1000 °C there are no big changes in the DSC trace only the endothermic peak positions were shifted towards right.

4.2.2 Phase identification (XRD analysis)

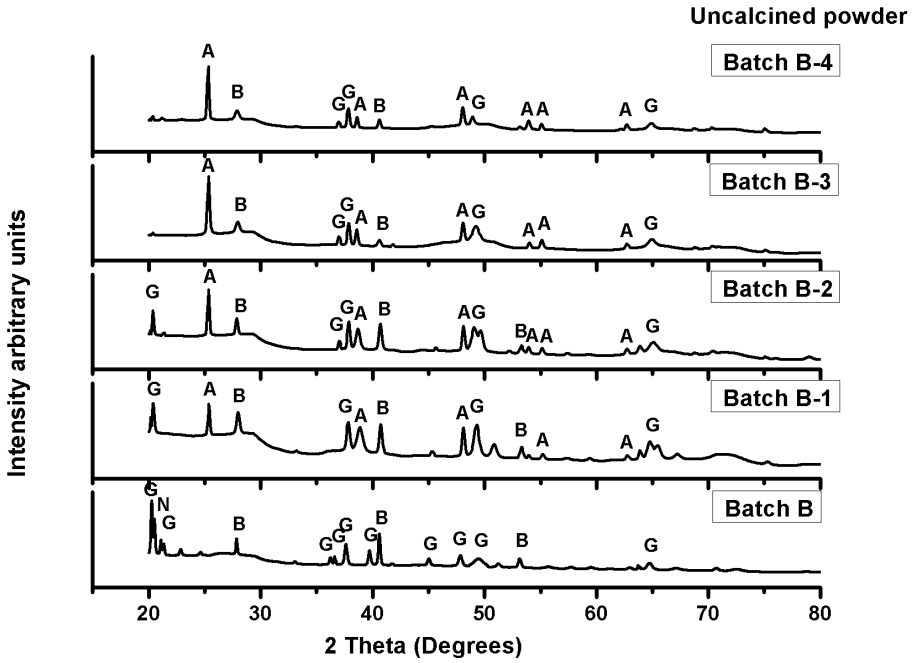

Figure 4.2.3 XRD patterns for uncalcined batches. (A- Anatase; G-Gibbsite; B-Bayerite).

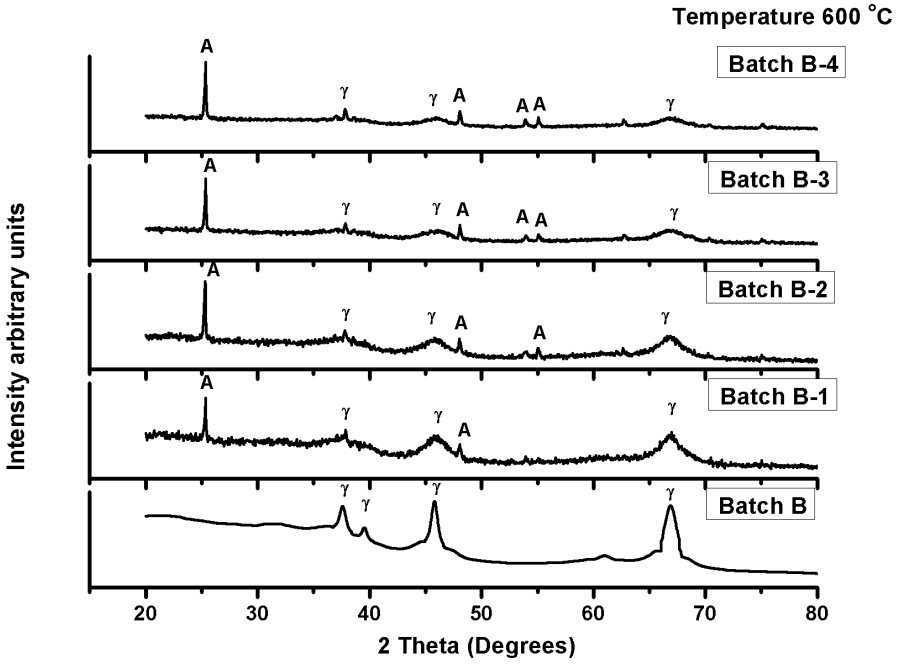

Figure 4.2.4 XRD patterns for 600 °C calcined batches. (A- Anatase; γ-Gamma Alumina).

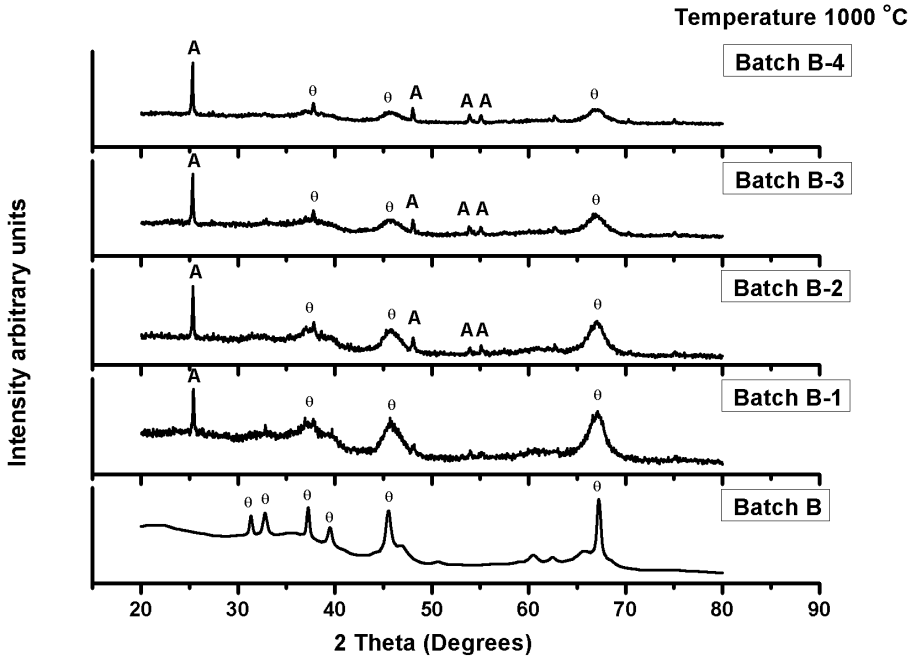

Figure 4.2.5 XRD patterns for 1000 °C calcined batches. (A- Anatase; θ-Theta Alumina).

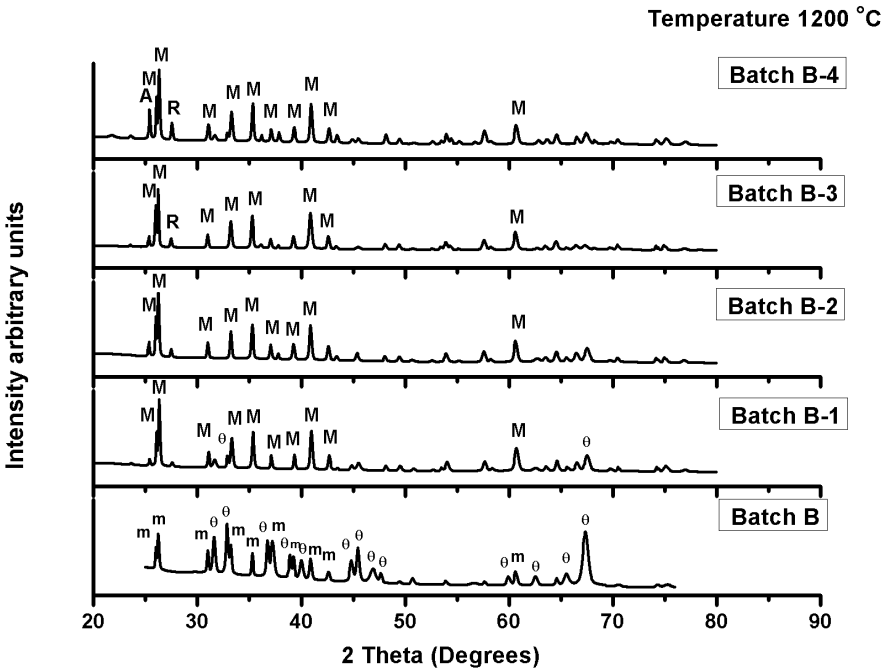

Figure 4.2.6 XRD patterns for 1200 °C calcined batches. (θ-Theta Alumina; m-Mullite; M-Mullite; A- Anatase; R- Rutile).

Figure 4.2.3, 4.2.4, 4.2.5 and 4.2.6 show the XRD plot of precursor powders and calcined powders of different batches. In each case, it is found that in the presence of TiO_2 additive new peaks for anatase phase developed and few transition alumina peaks disappear. With increasing wt % of TiO_2, peak intensity of anatase phase increases. Up to 1000 °C, in the presence of TiO_2 additive the major crystalline phases are anatase phase and transition alumina phases. At 1200 °C in the presence of TiO_2 additive, mullite is the major crystalline phase and the intensity of anatase peaks decreases. A new peak for rutile phases is developed for batch B-3. From the XRD results, it can be said that up to 1000 °C TiO_2 additive remains unreacted and at 1200 °C it started to disappear gradually with the progress of the mullite formation reaction. This phenomenon indicates the direct involvement of the additive in mullite phase formation process. Here two possibilities arise, one is the incorporation of Ti^{4+} in the transition alumina phase or the other is incorporation in amorphous silica. It is evident from the XRD plot that there is no peak shifting for transition alumina phases in the presence of TiO_2 additive up to 1200 °C which is contrary to the first assumption. On the other hand, it is already proved that tetrahedrally coordinated Ti^{4+} can substitute Si^{4+} from silica matrix up

to a limit of 11.5 wt % [4.30]. Therefore, it is possible that Ti first incorporates into the amorphous silica phase and helps to reduce the viscosity of the silica phase. This Ti incorporated silica phase in turn enhances the diffusion process or alumina dissolution thus helps mullite phase formation. This enhanced mullite phase formation is evident from figure 4.2.6. The Pauling radius of Si^{4+} and Ti^{4+} are 41pm and 56pm respectively [4.31]. The replacement of Si^{4+} by Ti^{4+} causes a residual strain and as a result mullite peak in a doped sample should be shifted to the left. This peak shifting is shown in figure 4.2.7.

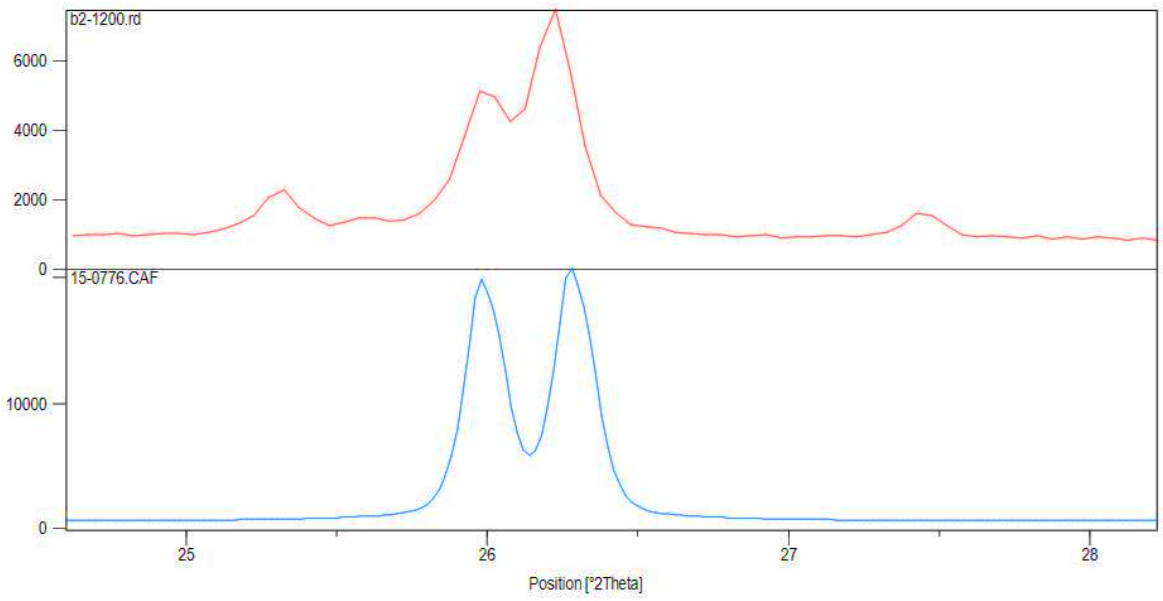

Figure 4.2.7 Peak shifting of batch B-2 calcined at 1200 °C (red) with reference file 15-0776 (blue)**.**

From figure 4.2.6 it can be said that in the presence of 3% additive the entire portion of the additive participated in mullite formation process, and there is no unreacted TiO_2 phase found. A small peak of transition alumina phase indicates the process of mullitization is yet to be complete. The presence of rutile phase in B-3 and B-4 batches indicates the limit of Ti^{4+} incorporation in mullite matrix for this type of diphasic powder lies in between 3-4.5%.

4.3 Sintering

The application of mullite as a potential structural ceramic could not be fully utilized due to the difficulty in attaining complete densification in absent of any additive. Solid state sintering of mullite precursor powder and the reaction sintering of silica, alumina mixture are the possible way to get higher densification. Solid state sintering requires higher temperature due to the lower rate of silicon and aluminium ion interdiffusion [4.32]. Here agglomerate formation during drying and calcination is another factor which affect densification. In reaction sintering two processes, reaction and densification occurs simultaneously and in most cases they are mutually favourable. But in case of mullite formation high activation enthalpy requirement makes the densification process difficult [4.33]. In case of monophasic gel, mullitization starts at lower temperature range around 980 °C but sintering occurs at higher temperature [4.34, 4.35]. If crystallization started before densification, then viscous flow sintering does not occur. Mullite formation requires higher activation enthalpy and for crystallization thermal energy is utilized, so densification is affected. In case of diphasic gel, mullite formation temperature is higher so densification initiate before crystallization and help sintering [4.36]. In this chapter, the effect of TiO_2 additive on densification process along with phase formation and microstructure of diphasic mullite precursor powder has been studied.

In case of diphasic precursor powder, two important factors on which densification depend are particle packing density and delayed crystallization. For higher particle packing density, a larger number of particles remains in contact with each other and the average curvature at the neck region increases which reduces the average diffusion distance, and better densification occurs. The delayed crystallization helps viscous flow sintering [4.36]. The viscosity of the siliceous amorphous phase decreases with increasing temperature and help densification before crystallization [4.32].

4.3.1 Densification study

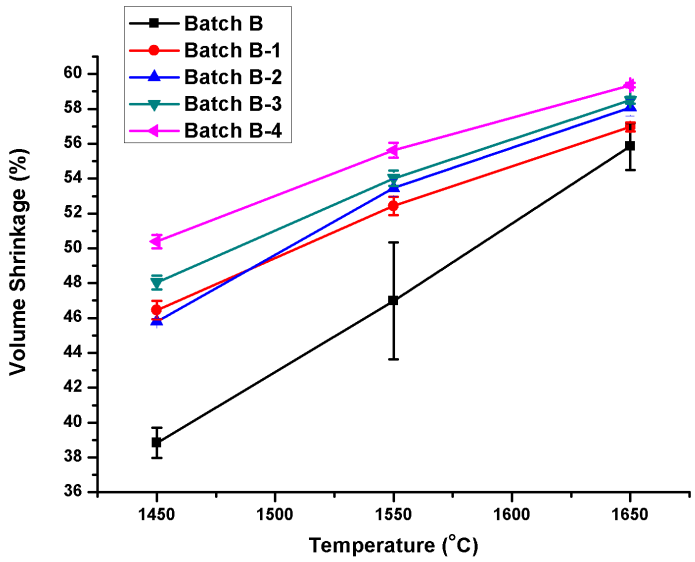

Figure 4.3.1 Variation of Volume Shrinkage with temperature.

Figure 4.3.1 shows the variation of % volume shrinkage with temperature for different batches. It is found from the graph that for all batches the % volume shrinkage increases as the sintering temperature rises from 1450 °C to 1650 °C. Comparing the curves of batch B with other TiO_2 containing batches (B-1 to B-4) it can be said that TiO_2 addition in mullite powder precursor leads to an increase in % volume shrinkage. The rising trend in volume shrinkage is due to the liquid phase formation and crystallization. In diphasic precursor, around 1200 °C mullitization process started and it requires high activation enthalpy so, the densification process hampered. In the presence of TiO_2 additive as the viscosity of the silica phases decreased, so the diffusion and mass transport become easier. This phenomenon helps densification which in turn causes volume shrinkage.

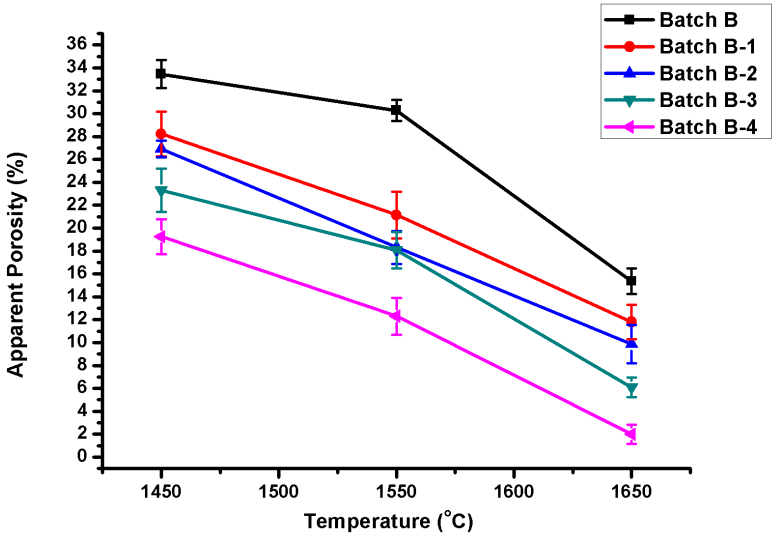

Figure 4.3.2 Variation of Apparent Porosity with temperature.

Figure 4.3.2 shows the variation of apparent porosity of different batches with temperature rise. From the figure, it can be said that the apparent porosity of the sintered batches is a direct function of sintering temperature and quantity of additive used. % apparent porosity is found to decrease both with rising temperature and increasing additive content.

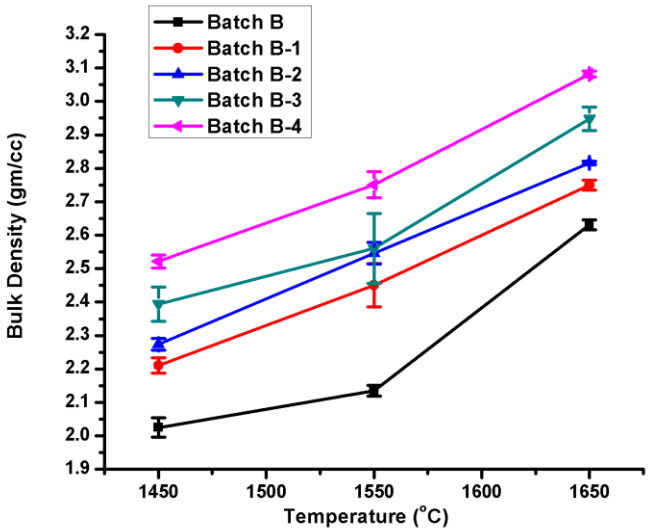

Figure 4.3.3 Variation of Bulk Density with temperature.

Bulk density is also found to increase almost linearly in TiO_2 doped sintered samples. TiO_2 as a sintering additive helps densification by two processes, one is forming liquid phase as mentioned earlier, and the other is substituting of Al^{3+} by Ti^{4+} followed by vacancy formation and enhanced mass transport. There are proofs for Al^{3+} replacement from its parent octahedral site in mullite structure by Ti^{4+} [4.37]. At a higher temperature in the presence of a greater amount of additive, it is expected both processes are occurring.

4.3.2 Flexure strength measurement

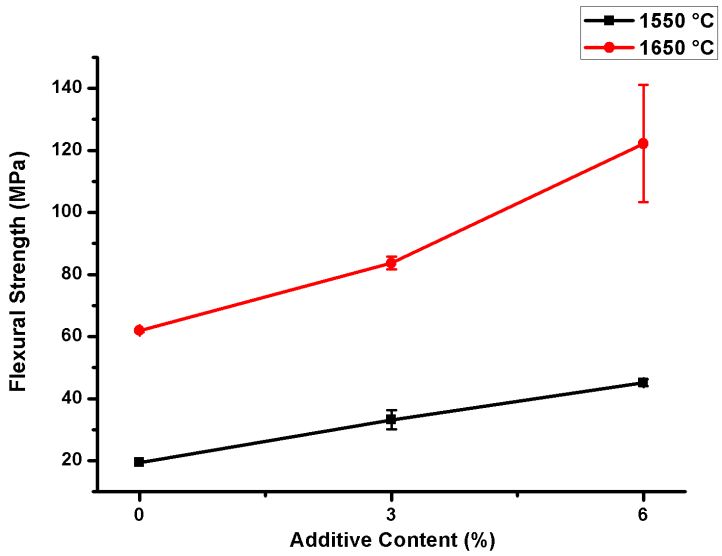

Figure 4.3.4 Variation of flexural strength with additive amount.

Figure 4.3.4 exhibit the flexural strength of batch B, B-2 and B-4 sintered at 1550 °C and 1650 °C. The marked increase in strength in 1650 °C sintered samples of different batches compared to the 1550 °C sintered samples of the corresponding batches is related to the lower porosity of the higher temperature fired batches [4.36].

4.3.3 Phases identification (XRD analysis)

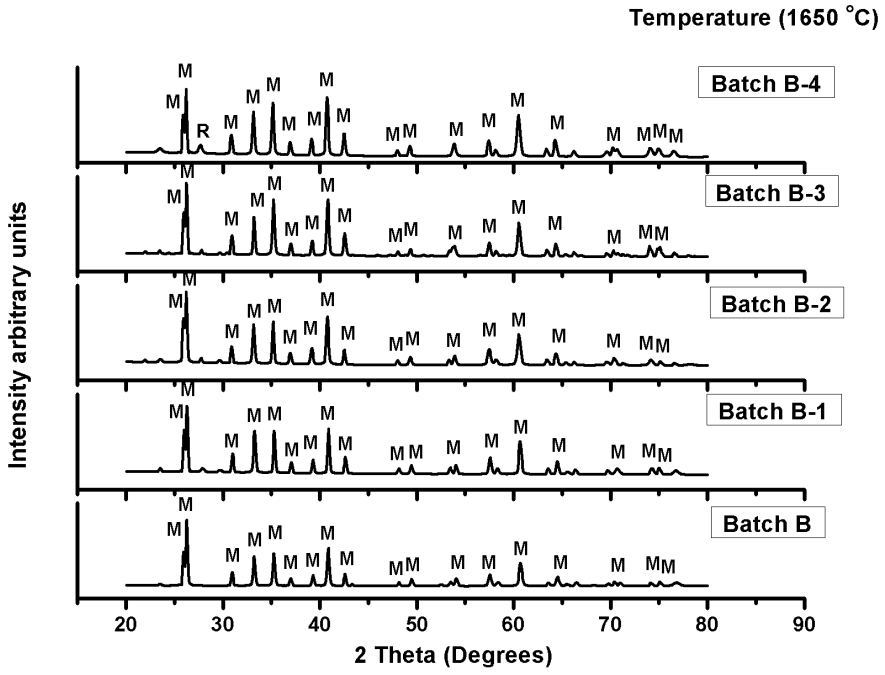

Figure 4.3.5 XRD patterns of 1650 °C sintered batches (M- Mullite; R- Rutile).

The XRD pattern of different batches fired at 1650 °C is shown in fig 4.3.5. From this figure it is obvious that the intensity of mullite peaks is increases as the quantum of additive increases. Thus it can be inferred that in this type of diphasic powder TiO_2 plays a favourable role in mullitization process. The presence of a small rutile peak for Batch B-4 indicates the solid solubility limit of Ti^{4+} in mullite matrix for this type of diphasic powder at a temperature 1650 °C is less than 6%. According to the SiO_2-Al_2O_3-TiO_2 ternary system phase diagram, when TiO_2 reaches its solid solution limit in mullite lattice then TiO_2 enters into the silica-rich glass phase. This low viscosity titania containing glass phase helps both the process of mullitization and sintering [4.38-4.40].

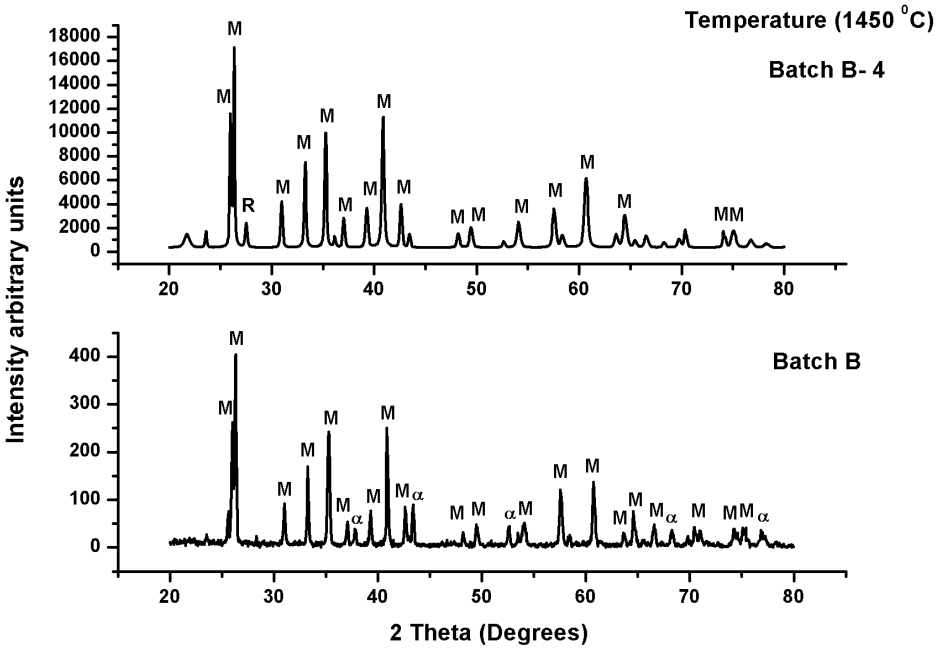

Figure 4.3.6 XRD patterns of batch-B and B-4 sintered at 1450 °C (M-Mullite; R- Rutile; α-Alpha alumina).

Samples of batch B fired at 1450 °C contain mullite phase as the main crystalline phase along with α-alumina phase. Samples of batch B-4 fired at the same temperature i.e.1450 °C contain mainly mullite phase as the crystalline phase. Here α-alumina phase is absent, and a small peak corresponding to rutile is found. In case of diphasic precursor, it is found that after nucleation, the growth of mullite crystals occurs through the siliceous phase. Sometimes alumina particles can get entrapped by the growing mullite grain. The diffusion of this entrapped alumina through the mullite grain towards siliceous matrix is difficult [4.41]. Therefore, α-alumina phase is found to be present in batch B. In presence of TiO_2 additive, as the additive helps in alumina dissolution process by reducing the viscosity of silica phase so α-alumina phase is absent here. The intensified mullite peaks in the presence of TiO_2 demonstrate the supportive role of this additive in mullitization process.

4.3.4 Microstructure analysis (FESEM)

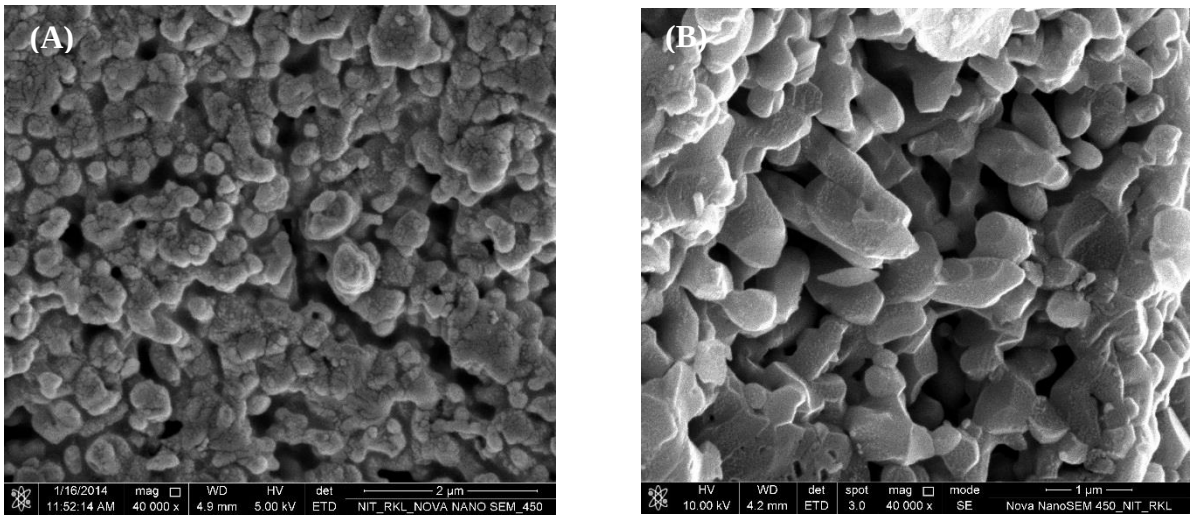

Figure 4.3.7 FESEM micrograph of 1450 °C sintered samples: (A) batch B (B) batch B-4.

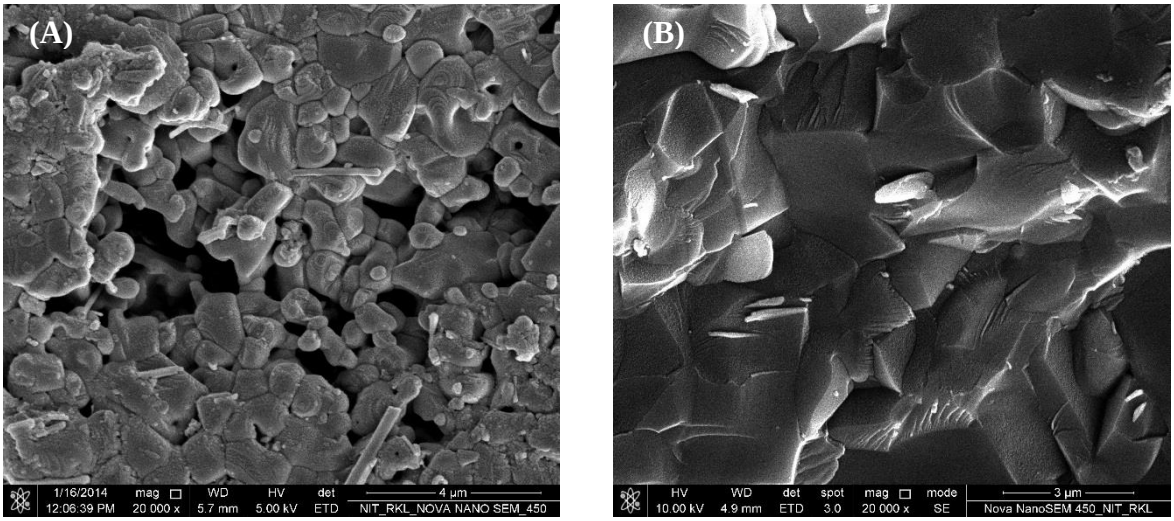

Figure 4.3.8 FESEM micrograph of 1650 °C sintered samples: (A) batch B (B) batch B-4.

The microstructure of 1450 °C and 1650 °C fired samples of batch B, and B-4 is shown in figure 4.3.7 and 4.3.8 respectively. The micrograph of batch B exhibit cluster of grains and pores. At higher temperature, it is found that within the cluster the grains are equiaxed and dense. In batch B-4 at 1450 °C densification started and grain to grain bonding is clearly visible. Grain impingement is another factor this is found in this case. In the presence of TiO_2

at 1650 °C highly densified microstructure is observed. High theoretical density achievement and better strength of B-4 batch are also supported by this type of micrograph.

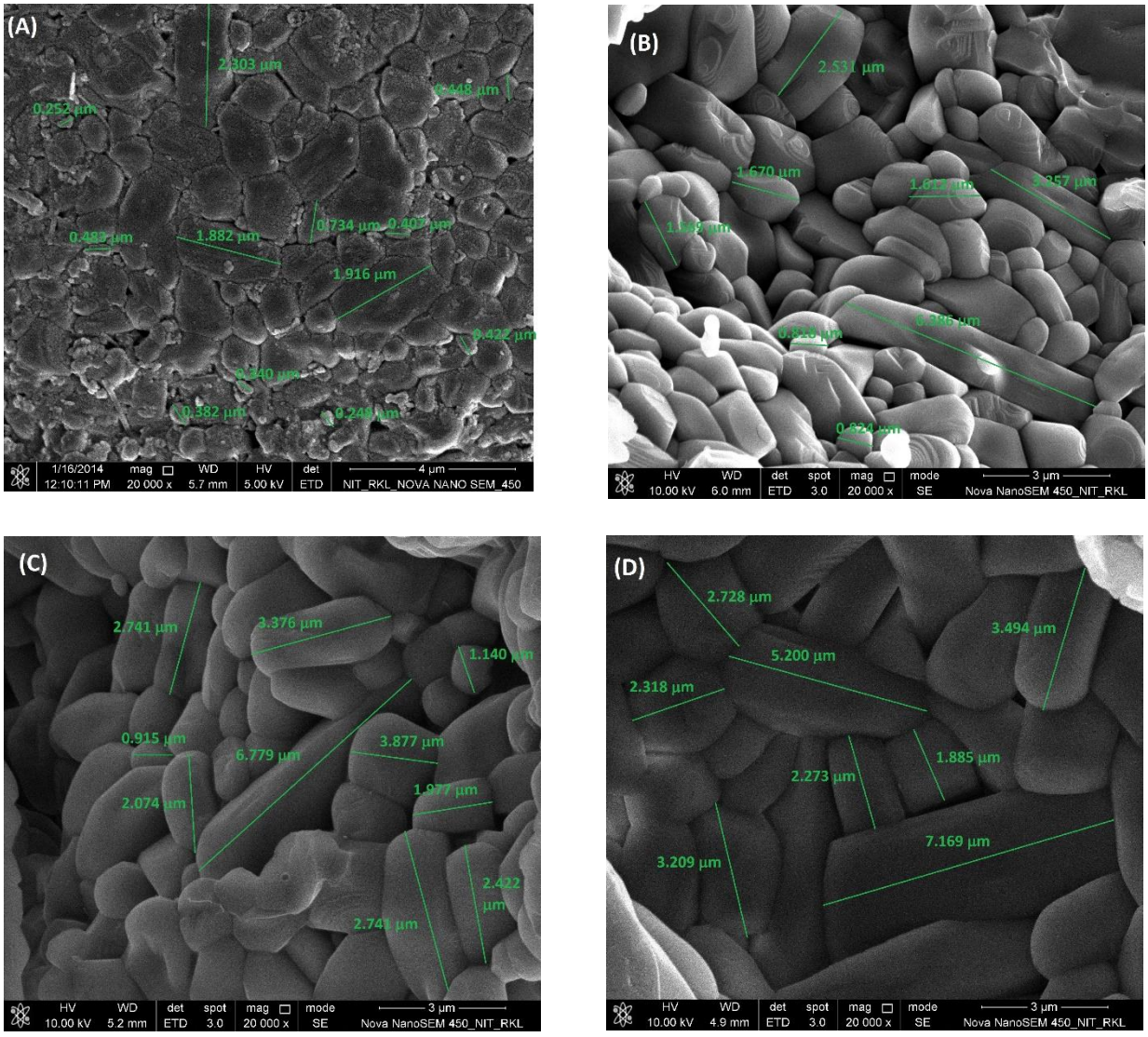

Figure 4.3.9 FESEM micrograph of 1650 °C sintered samples: (A) batch B (B) batch B-1 (C) batch B-2 (D) batch B-4.

Table-3.5 Average grain size.

Batch	**Min μm**	**Max μm**	**Mean μm**
Batch B	0.338	2.303	0.924
Batch B-1	0.818	6.386	1.759
Batch B-3	0.915	6.779	2.117
Batch B-4	1.684	7.169	3.161

The effect of TiO_2 additive concentration on microstructure and grain morphology is shown in figure 4.3.9. Here all samples are 1650 °C fired, and they contain the TiO_2 additive in the range 0-6%. The undoped samples of batch B exhibit equiaxed grains of two different sizes; one is larger (2μm), and the other is smaller (less than 1μm). In doped samples, microstructures show a duplex nature i.e., some equiaxed grains along with some elongated grains. As the dopant concentration increases from 1.5% to 6 %, the number of equiaxed grains decreases and the elongated grain increases. In batch B-4 grain growth and anisotropy is maximum. The average grain size in each batch is measured using image-J software and the min, max and average grain size of batch B, B-1, B-3 and B-4 are given in table 3.5. From the table it is clear that with increasing the concentration of TiO_2 additive the grain size is also increases. Grain anisotropy is generally favoured by the presence of liquid phase. In diphasic powder in presence of higher amount of additive, the formation kinetics of the titanium-doped mullite solid solutions is slow therefore some unreacted dopant remains in the sample which reduces the viscosity of the residual silica reach phase and help anisotropic grain growth [4.40].

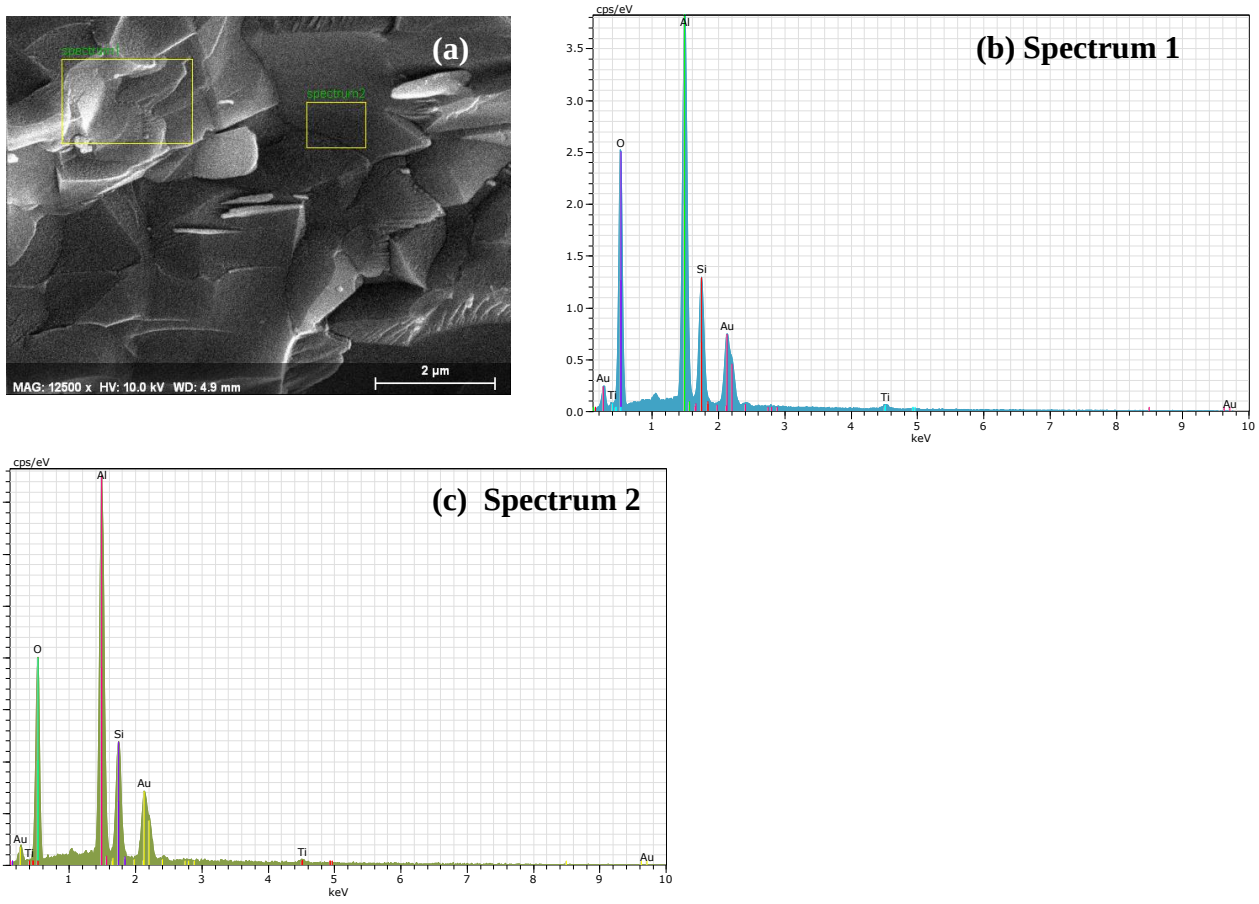

Figure 4.3.10 FESEM micrograph of batch-B4 fired at 1650 °C along with EDS spectrum of mullite grains (a) FESEM micrograph (b) spectrum 1 (c) spectrum 2.

The TiO_2 incorporation in the mullite matrix is analysed by the EDS study. The EDS spectrum of the mullite grains, as shown in figure 4.3.10, shows the presence of Al, Si, O, and Ti. The uniform distribution of dopant in the mullite phases is also confirmed by mapping the distribution of previously defined elements over the scanned area.

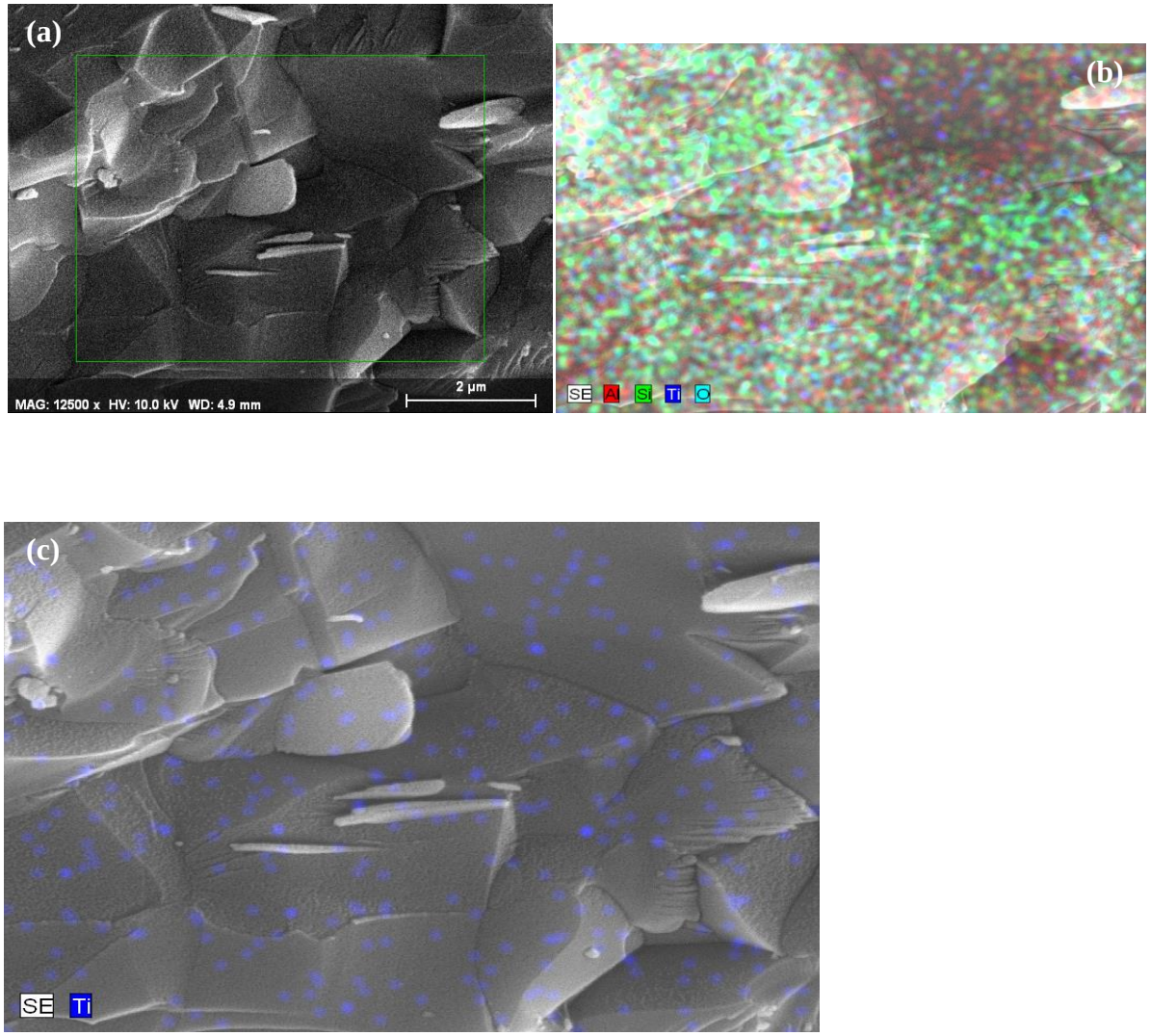

Figure 4.3.11 Image analysis of batch-B4 fired at 1650 °C (a) FESEM micrograph, (b) Distribution of all elements, (c) Distribution of Titania

References:

[4.1] E. Tkalcec, S. Kurajica, H. Ivankovic, Diphasic aluminosilicate gels with two stage mullitization in temperature range of 1200-1300 ˚C, Journal of the European Ceramic Society, 25 (2005) 613–626.

[4.2] S. Bhattacharyya, T. K. Mukhopadhyay, K. Dana, S. Ghatak, Pressureless reaction sintering of yttrium aluminium garnet (YAG) from powder precursor in the hydroxyhydrogel form, Ceramics International, 37 [8] (2011) 3463-3468.

[4.3] S. R. Raghavan, H. J. Walls, S. A. Khan, Rheology of silica dispersion in organic liquids: new evidence for solvation forces dictated by hydrogen bonding, Langmuir, 16 (2000) 7920-7930.

[4.4] H. Kamiya, M. Mitsui, H. Takano, S. Miyazawa, Influence of particle diameter on surface silanol structure, hydration forces, and aggregation behavior of alkoxide-derived silica particles, J. Am. Ceram. Soc., 83 [2] (2000) 287–293.

[4.5] U. Paik, J. P. Kim, Y. S. Jung, Y. G. Jung, T. Katoh and J. G. Park, V. A. Hackley, The effect of Si dissolution on the stability of silica particles and its influence on chemical mechanical polishing for interlayer dielectrics, Journal of the Korean Physical Society, 39 (2001) S201-S204.

[4.6] C. C. Osawa and C. A. Bertran, Mullite formation from mixtures of alumina and silica sols: mechanism and pH effect, J. Braz. Chem. Soc. 16 [2] (2005) 251-258.

[4.7] S. Bhattacharyya, S. Ghatak, Synthesis and characterization of YAG precursor powder in the hydroxyhydrogel form, Ceramics International, 35 [1] (2009) 29-34.

[4.8] J. Temuujin, K. Okada, K.J.D. Mackenzie, Effect of mechanochemical treatment on the crystallization behaviour of diphasic mullite gel, Ceramics International, 25 (1999) 85-90.

[4.9] X. H. Jin, L. Gao, J. K. Guo, The structural change of diphasic mullite gel studied by XRD and IR spectrum analysis, Journal of European Ceramic Socity, 22 (2002) 1307-1311.

[4.10] J. E. Lee, J. W. Kim, Y. G. Jung, U. Paik, Effect of precursor pH and composition on the grain morphology and size of mullite ceramics in aqueous system, Materials Letters, 57 (2003) 3239-3244.

[4.11] A. K. Chakraborty, Reinvestigation of Al–Si Spinel Phase in Diphasic Al_2O_3–SiO_2 Gel Journal of the American Ceramic Society, 88 [1] (2005)134–140.

[4.12] B. E. Yoldas, Microstructure of monolithic materials formed by heat treatment of chemically polymerised precursor in the Al_2O_3-SiO_2 binary, Am. Ceram. Soc. Bull., 59 [4] (1980) 479-83.

[4.13] T. Horiuchi, T. Sugiyama, and T. Mori, Factors for Maintenance of a High Surface Area of Silica-Coated α-Alumina after Heating >1573 K, J. Mater. Chem., 3 [8] (1993) 861-65.

[4.14] F. T. Wallenberger, J. B. MacChesney, R. Naslain, H. D. Ackler, Avanced Inorganic Fibers: Processes-Structure-Properties-Applications, Materials technology series, 6 (1999).

[4.15] Y. Saito, T. Takei, S. Hayashi, A. Yasumori, and K. Okada, Effects of Amorphous and Crystalline SiO_2 Additives on γ-Al_2O_3-to-α-Al_2O_3 Phase Transitions, J. Am. Ceram. Soc., 81 [8] (1998) 2197–200.

[4.16] K. Okada, N. Otsuka, Characterization of the spinel phase from SiO_2–Al_2O_3 xerogels and the formation process of mullite, J. Am. Ceram. Soc., 69 [9] (1986) 652–656.

[4.17] X. H. Jin, L. Gao, J. K. Guo, The structural change of diphasic mullite gel studied by XRD and IR spectrum analysis, J. Eur. Ceram. Soc., 22 (2002) 1307-1311.

[4.18] H. Schneider, D. Voll, B. Saruhan, M. Schmucker, T. Schaller, A. Sebald, Constitution of the γ-alumina phase in chemically produced mullite precursors, J. Eur. Ceram. Soc. 13 (1994) 441–448.

[4.19] G. M. Anilkumar, P. Mukundan, A. D. Damodaran, K. G. W. Warrier, Effect of precursor pH on the formation characteristics of sol–gel mullite, Mater. Lett. 33 (1997) 117-122.

[4.20] R. Singh, S. Bhattacharyya, Synthesis of Mullite Precursor Powder in Diphasic Gel Form, Trans. Ind. Ceram. Soc., 73 [2] (2014) 98-101.

[4.21] D. Voll, A. Berana, H. Schneider, Temperature-dependent dehydration of sol-gel-derived mullite precursors: An FTIR spectroscopic study, Journal of the European Ceramic Society, 18 (1998) 1101-1106.

[4.22] P. Padmaja, G. M. Anilkumar, P. Mukundan, G. Aruldhas, K.G.K. Warrier, Characterisation of stoichiometric sol–gel mullite by fourier transform infrared spectroscopy, International Journal of Inorganic Materials, 3 (2001) 693–698.

[4.23] J. E. Lee, J. W. Kim, Y. G. Jung, C. Y. Jo, U. Paik, Effects of precursor pH and sintering temperature on synthesizing and morphology of sol–gel processed mullite, Ceramics International, 28 (2002) 935–940.

[4.24] K. Hellgardt, D. Chadwick, Effect of pH of precipitation on the preparation of high surface area aluminas from nitrate solutions, Ind. Eng. Chem. Res., 37 (1998) 405-411.

[4.25] C. C. Lin and P. Y. Shen, The role of Ti^{+4} on the structure and transformations of gel-produced Zn2SiO4, J. Solid State Chem., 112 (1994) 381–386.

[4.26] M. C. Wang, The effect of TiO2 addition on the preparation and phase transformation for precursor -spodumene powders. J. Mater. Res., 9 (1994) 2290-2297.

[4.27] E. R. de Sola, F. Estevan, J. Alarcon, Low-temperature Ti containing 3:2 and 2:1 mullite nanocrystals from single-phase gels, Journal of the European Ceramic Society, 27 (2007) 2655–2663.

[4.28] S. Sundaresan and I. A. Aksay, Mullitization of Diphasic Aluminosilicate Gels, J. Am. Ceram. Soc., 74 [10] (1991) 2388-92.

[4.29] D. X. Li and W. J. Thomson, Kinetic Mechanisms for Mullite Formation from Sol–Gel Precursors, J. Mater. Res., **5** [9] (1990) 1963-69.

[4.30] C. J. Brinker and G. W. Scherer, Sol–Gel Science, The Physics and Chemistry of Sol-Gel Processing, Academic Press, New York, 1990.

[4.31] Web Elements Periodic Table: the periodic table on the web, available at "www.webelements.com".

[4.32] F. Kara and J. A. Little, Sintering behaviour of precursor mullite powders and resultant microstructures, Journal of the European Ceramic Society, 16 (1996) 627-635.

[4.33] P. D. D Rodrigo and P. Boch, High purity mullite ceramics by reaction sintering, Int. J. High Technology Ceramics, 1 (1985) 3-30.

[4.34] B. E. Yoldas, Microstructure of Monolithic Materials Formed by Heat Treatment of Chemically Polymerized Precursors in the Al.sub.2 O.sub.3--SiO.sub.2 Binary, Ceramic Bulletin, 59 [4] (1980), 479-83.

[4.35] K. Okada and N. Otslka, Change in chemical composition of mullite formed from $2SiO_2.3Al_2O_3$ xerogel during the formation process, J. Am. Ceramic Soc., 70 [10] (1987) C245-C247.

[4.36] T. Ebadzadeh, Formation of mullite from precursor powder: sintering, microstructure and mechanical properties, Materials Science and Engineering, A355 (2003) 56-61.

[4.37] C. Baudin and J. S. Moya, Influence of titanium oxide on the sintering and microstructural evolution of mullite, J. Am. Ceram. Soc., 67 (1984) C134–C136.

[4.38] H. S. Tripathi, G. Banerjee, Synthesis and mechanical properties of mullite from beach sand sillimanite: effect of TiO2, J. Eur. Ceram. Soc., 18 (1998) 2081–2087.

[4.39] S. H. Hong and G. L. Messing, Mullite transformation kinetics in P_2O_5, TiO_2 and B_2O_3-doped aluminosilicate gels, J. Am. Ceram. Soc., 80 [6] (1997) 1551-1559.

[4.40] E. R. de Sola, F. J. Serrano, E. D. Pinar, M. M. Reventos, A. I. Pardo, M. A. Kojdecki, J. M. Amigo, J. Alarcon, Solubility and microstructural development of TiO_2-containing $3Al_2O_3{\cdot}2SiO_2$ and $2Al_2O_3{\cdot}SiO_2$ mullites obtained from single-phase gels, Journal of the European Ceramic Society 27 (2007) 2647–2654.

[4.41] L. B. Kong, T. S. Zhang. J. Ma, F. Boey, R.F. Zhang, Mullite phase formation in oxide mixtures in the presence of Y_2O_3, La_2O_3 and CeO_2, Journal of alloy and compounds, 372 (2004) 290-299.

CHAPTER 5

CONCLUSIONS AND SCOPE OF FUTURE WORK.

5.1 Conclusion

For the fulfilment of research objective, the work plan was outlined and accordingly several steps successfully performed. The research work included in this thesis can be divided into two parts. The first part related with the synthesis and the characterization of diphasic mullite precursor powder. The precursor powder synthesised both in presence and in absence of sintering additive is discussed here. The effect of solution pH on the properties of the prepared mullite powder is also included. The second part deals with the sintering of the prepared powder precursor. The characterization study of the sintered pellets to find out the effect of TiO_2 additive on densification is also covered in this part. The outcomes of this study are summarized as follows:-

- Diphasic mullite precursor powder can be successfully prepared by reverse addition technique using aluminium nitrate and fumed silica as starting material and ammonia as the precipitant.
- The effect of solution pH on the properties of this diphasic mullite precursor powder has been studied. It is found from the study that the surface area, primary particle size, agglomerate formation and thermal decomposition are very much affected by the change of solution pH during precipitation. Mullite powder prepared at pH-8 exhibit better properties.
- The mullite phase formation and densification of the diphasic powder is enhanced in the presence of TiO_2 additive. Maximum density, higher strength and minimum porosity is found in B4 batch i.e. in the presence of 6% TiO_2 additive.
- The XRD study revealed that there is no aluminium titanate phase formation occurred during calcinations and densification.
- The microstructure of the sintered samples and the grain morphology is also affected by the addition of TiO_2 additive.

- Some elongated grains are found along with the equiaxed grains in the doped samples. In batch B-4 grain growth and anisotropy is maximum.

Therefore, it can be inferred that in presence of 6% TiO_2 additive, maintaining precipitation pH around 8, reverse addition method is a suitable method for obtaining highly densified mullite with other positive properties.

5.2 Scope of future work

- ✓ The theoretical density achieved in this process is greater than 97.5%. Further modification in this theoretical density achievement can be tried by using other liquid forming additive.
- ✓ The effect of particle size of the sintering additive on densification behaviour can be done.
- ✓ A detailed study on the quantitative phase analysis can be done to find out the actual amount of mullite formed in different batches.

Publications

Paper published:

1. **Rupali Singh** & Sunipa Bhattacharyya, Synthesis of Mullite Precursor Powder in Diphasic Gel Form, Trans. Ind. Ceram. Soc., vol. 73, no. 2, pp. 98-101 (2014).

Paper communicated:

1. **Rupali Singh** & Sunipa Bhattacharyya, Effect of solution pH on mullite phase formation from a diphasic precursor powder, under reviwe in Journal of the Australian Ceramic Society.

Conference:

1. **Rupali Singh** & Sunipa Bhattacharyya, Synthesis of Mullite Precursor Powder in Hydroxyhydrogel Form. In: International Conference on Ceramic Science on occasion of 77th Annual Session of The Indian Ceramic Society, Jamshedpur, India, 19-20th December 2013.
2. **Rupali Singh** & Sunipa Bhattacharyya, Sintering Behaviour Of Mullite Precursor Powder Prepared In The Diphasic Gel Form. In: 6^{th} International Symposium for Research Scholars 2014 IIT Madras, Chennai, India, 11-13 December 2014.

Curriculum Vitae

Rupali Singh
D/O: Nayantara Singh
130/77 Naina Niwas, Near Gita Vatika,
Shahpur, Gorakhpur,
Uttar Pradesh (273006) India.
Email: rupali18feb@gmail.com
Mobile: 9692913328, 9453474011
Date of Birth: 18.07.1991

Education: Bachelor of Technology (Mechanical Engineering), U.P.T.U, 2011.
Master of Technology (Research) (Ceramic Engineering) NIT Rourkela, Thesis submitted.

Experience: 6 Months of Teaching Experience at Shivajirao S. Jondhle College of Engineering and Technology (Maharashtra), 2012.

Publication and Conferences:

Paper published:

1. **Rupali Singh** & Sunipa Bhattacharyya, Synthesis of Mullite Precursor Powder in Diphasic Gel Form, Trans. Ind. Ceram. Soc., vol. 73, no. 2, pp. 98-101 (2014).

Paper communicated:

1. **Rupali Singh** & Sunipa Bhattacharyya, Effect of solution pH on mullite phase formation from a diphasic precursor powder, under reviwe in Journal of the Australian Ceramic Society.

Conferences:

1. **Rupali Singh** & Sunipa Bhattacharyya, Synthesis of Mullite Precursor Powder in Hydroxyhydrogel Form. In: International Conference on Ceramic Science on occasion of 77th Annual Session of The Indian Ceramic Society, Jamshedpur, India, 19-20th December 2013.

2. **Rupali Singh** & Sunipa Bhattacharyya, Sintering Behaviour Of Mullite Precursor Powder Prepared In The Diphasic Gel Form. In: 6th International Symposium for Research Scholars 2014 IIT Madras, Chennai, India, 11-13 December 2014.